

# Puckering Free Energy of Pyranoses: an NMR and Metadynamics–Umbrella Sampling Investigation

E. Autieri, M. Sega,\* and F. Pederiva

*Department of Physics and I.N.F.N., University of Trento,  
via Sommarive 14, 38123 Trento, Italy*

G. Guella

*Department of Physics, University of Trento,  
via Sommarive 14, 38123 Trento, Italy*

## Abstract

We present the results of a combined metadynamics–umbrella sampling investigation of the puckered conformers of pyranoses described using the GROMOS 45a4 force field. The free energy landscape of Cremer–Pople puckering coordinates has been calculated for the whole series of  $\alpha$  and  $\beta$  aldohexoses, showing that the current force field parameters fail in reproducing proper puckering free energy differences between chair conformers. We suggest a modification to the GROMOS 45a4 parameter set which improves considerably the agreement of simulation results with theoretical and experimental estimates of puckering free energies. We also report on the experimental measurement of altrose conformers populations by means of NMR spectroscopy, which show good agreement with the predictions of current theoretical models.

## I. INTRODUCTION

Within the framework of classical force fields, the number of computer experiments on saccharides has grown considerably in recent years, and various systems have been addressed<sup>1–27</sup>. Devising a realistic model of monosaccharides is obviously a decisive step in order for carbohydrates simulations to have enough predictive power. The accurate description of monosaccharides with classical force fields is not an easy task, because of the delicate interplay of different factors such as the presence of a high number of intramolecular hydrogen bonds, the competition of these hydrogen bonds with water-sugar ones and important steric and electrostatic effects between ring substituents in spatial proximity (see for example Ref. 28 and references within). The problem of reproducing some carbohydrates peculiarities, such as the rotameric distribution of the hydroxymethyl group or the anomeric and exo-anomeric effects, have been addressed in various force fields, and the reader can find some comparative analyses in Refs. 29–31. However, considerably less attention has been devoted so far to the correct reproduction of the ring conformational properties.

Cyclic monosaccharides can appear indeed as puckered rings, and their conformational transitions dramatically alter the equilibrium properties of both single sugar rings as well as those in oligo and polysaccharides<sup>32</sup>. Despite the large number of possible puckered conformers, many biologically relevant monosaccharides in the pyranoid form appear almost always in one stable puckered conformation, the second most populated state being so unlikely not to be detectable by actual experimental techniques. In spite of that, several authors reported an inappropriately high percentage of secondary puckered conformations<sup>32–37</sup> when modeling carbohydrates using classical force fields such as GROMOS<sup>34,35,38–41</sup> or OPLS-AA<sup>42</sup> for simulations of sugars in solution. Regarding the latest GROMOS parameter set for carbohydrates (45a4)<sup>35</sup>, non-chair conformers have been shown to be accessible during equilibrium simulation runs of  $\beta$ -D-glucose<sup>28</sup>, and two recent works<sup>43,44</sup> estimated the free energy difference between chair conformers to be at least 10 kJ/mol lower than most theoretical and ab-initio simulation results. Besides equilibrium simulations, the importance of ring puckering has been proven by simulated pulling experiments, employed to interpret single molecule force-spectroscopy data<sup>21,45,46</sup>. In this case, ring conformational transitions simulated using three different force fields (AMBER94<sup>47</sup>, AMBER-GLYCAM<sup>48</sup> and CHARMM-Parm22/SU01<sup>49</sup>) led to different interpretation of the same experimental data<sup>21</sup>. Having control on the reli-

ability of force fields in reproducing puckering properties would certainly improve the predictivity of computer simulations of saccharides.

It is hence understandable how desirable is a reparametrization of those force fields which present unphysical ring conformers. This difficult task, however, is made even more arduous by the lack of experimental estimates of conformers populations, as the only monosaccharide investigated so far is idose<sup>50</sup>. This work aims at filling, at least partially, these gaps. On one hand we estimated the chair conformers populations of altrose, obtained from the assignment of its <sup>1</sup>H NMR spectrum. On the other hand, we performed a combined metadynamics – umbrella sampling investigation<sup>51</sup> of the puckering properties of all  $\alpha$  and  $\beta$ -D-aldopyranoses, modeled using the GROMOS 45a4 parameter set<sup>35</sup>, and identified a new set of parameters that satisfactorily reproduces the puckering free energies of the main ring conformers.

This paper is organized as follows: in Sec. II the problems related to the determination of puckering free energy landscape will be presented; in Sec. III the results of an NMR investigation of altropyranose conformers populations are presented; in Sec. IV the combined metadynamics–umbrella sampling will be discussed, as well as the use of Cremer–Pople puckering coordinates<sup>52,53</sup>, their peculiarities as collective variables, and the simulation details; in Sec. V the puckering free energy profile obtained with the GROMOS 45a4 force field for  $\beta$ -D-glucose is discussed in detail and compared to recent similar calculations<sup>43,44</sup>. In Sec VI we present the puckering free energy profiles of the whole  $\alpha$  and  $\beta$  series of D-aldohexoses modeled with the GROMOS 45a4 force field, showing that the puckering free energies are so poorly reproduced, that the inverted chair conformers of galactose, mannose and  $\alpha$ -D-Glc become significantly populated. Subsequently, we propose a change to the 45a4 parameter set, showing how the free energies obtained with the use of the new parameter set compare favorably with available theoretical and experimental data. Eventually, some concluding remarks are presented in Sec. VII.

## II. THE PROBLEM OF PYRANOSSES PUCKERING FREE ENERGY

In this work we are focusing on a particular class of carbohydrates, namely, aldohexoses, saccharides of composition  $C_6H_{12}O_6$ . Aldohexoses can appear in nature in the form of six-membered, cyclic rings, conventionally known as the pyranose form. Pyranoses are characterized by the presence of five chiral centers located at the five ring carbon atoms. Following

the convention of Fig. 1, these chiral carbons are here denoted as C1 (the anomeric carbon atom), C2, C3, C4 and C5 (the configurational carbon atom). This leads to quite a high number ( $2^5 = 32$ ) of diastereoisomers, characterized by the axial or equatorial orientation of ring substituents. Based on the chirality at C1 and C5 it is possible to classify pyranoses into  $\alpha$ - and  $\beta$ -pyranoses or L- and D-pyranoses, respectively<sup>54</sup>. For example,  $\alpha$ -D-Glc and  $\beta$ -L-Glc differ from  $\beta$ -D-Glc only by the chirality at C1 and C5, respectively.

For each of these two chiralities,  $2^3 = 8$  stereoisomers remain, which are conventionally named<sup>54</sup> glucose (Glc), galactose (Gal), mannose (Man), allose (All), altrose (Alt), talose (Tal), gulose (Gul) and idose (Ido). The position of substituents at the chiral centres are reported for convenience in Tab. I, for  $\beta$ -D-aldopyranoses.

Each of these stereoisomers, in turn, can adopt different ring conformations. According to IUPAC recommendations<sup>55</sup>, the conformation with two parallel ring sides (four coplanar atoms) and the other two atoms at opposite side of the ring plane is called *chair*. Chair conformers occur in two forms: the one with C4 and C1 respectively above and below the plane defined by the other four atoms, is identified by the symbol  ${}^4C_1$ , while the conformer showing C1 above the ring plane and C4 below it is denoted by the symbol  ${}^1C_4$  and often called *inverted chair*. Other puckered conformers with four coplanar atoms exist, such as the so-called *boat* and *skew-boat* (the latter also known as *twist-boat*). In the case of boats, two parallel ring sides define the ring plane and the atoms at the extrema of the ring are either above or below the ring plane (indicated for examples as  ${}^3,0B$  or  $B_{3,0}$ ); in the case of skew-boats the ring plane is defined by three adjacent atoms and the nonadjacent one with the other ring atoms at opposite side of the ring plane (e.g.  ${}^3S_1$ ). Fig. 2 depicts a simplified stereoprojection of the conformation globe<sup>56</sup> of a 6-membered ring spanned by the spherical coordinates  $Q, \theta, \phi$  where the puckering amplitude  $Q$  in this work is averaged out during the sampling phase. By considering  $\theta \in (0, \pi)$ , the globe surface can be projected into a rectangular form, which is one of the commonly employed representation of Cremer–Pople coordinates<sup>57</sup>. The 0 and  $\pi$  values of  $\theta$  present in Fig. 2 (where the chair forms are put outside the plane to underline this) and in subsequent plots are left so that the span of  $\theta$  is clear.

Many of the possible conformations are not likely to contribute significantly to the chemistry and physics of monosaccharides. For pyranoses, only the  ${}^4C_1$  and  ${}^1C_4$  conformations happen to be eligible to be the most stable conformations, that is, global minima which are

well separated in energy from neighbouring local ones. Other conformers such as boats and skew-boats can in principle appear as local, scarcely populated minima.

The concept of puckering in rings (specifically, in six-membered rings) dates back to the studies of Sachse<sup>58,59</sup> on cyclohexane in the late nineteenth century, and has been later applied also to saccharidic rings<sup>60</sup>. Although it was clear that the most stable conformers could have been only either of the two chairs, lack of quantitative information on their relative abundance stimulated many theoretical approaches (for an historical review the reader can look at Ref. 57). A quantitative estimate of the free energy difference between puckered conformers in aqueous solution (and not, as it is sometimes erroneously reported, in vacuum) came first with the analysis performed by Angyal who assigned, employing an empirical scheme, specific free energy contributions to different destabilizing interactions. The various terms were derived from measured equilibria in solution of cyclitols with their borate complexes<sup>61</sup>. Later, employing a molecular-mechanical approach, Vijayalakshmi and Rao<sup>62</sup> obtained other estimates, which were anyway compatible with the inverted chair free energies predicted by Angyal.

Semiempirical methods have been in general a quite successful approach for determining the stereochemical properties of numerous cyclic compounds<sup>63</sup>. Unfortunately, experimental estimates of the ring conformational free energy are not feasible for many pyranoses, mostly because the populations of the less stable conformers are usually too tiny to be detected with probes such as NMR<sup>64,65</sup>. For some pyranoses, however, the destabilizing effects in the  ${}^4C_1$  and  ${}^1C_4$  conformations are similar and, as in the case of idose, the relative population of these two conformers becomes an experimentally accessible quantity. Indeed, the free energy differences for idose reported in Refs. 61 and 62 resulted to be in agreement with the experimental findings obtained by Snyder and Serianni years later<sup>50</sup>. The agreement with experiment is within  $\simeq 4\text{kJ/mol}$ , but these results are of particular significance because they correctly predicted the preference of  $\alpha$ -D-Ido for the inverted chair conformer. Except for -D-Alt and, possibly, -D-Gul, only lower bounds can in principle be determined, given the sensitivity of NMR measurements. In this sense, anyway, semiempirical methods predict correctly the extremely high free energy of inverted chairs of glucose, galactose and mannose.

Some recent experiments involving atomic force microscope (AFM) spectroscopy have allowed researchers to estimate the puckering free energy of conformers different from the chair ones. Marszalek, Lee, and coworkers<sup>45,66,67</sup>, for example, estimated the puckering free

energy of glucose twisted boats employing AFM pulling on dextran, cellulose, and pustulan. These polysaccharides are all homopolymers of glucose but in the elongation process, due to the different linkages, cellulose presents (apart from chain flexibility) only ring deformation, while pustulan presents both ring deformation and rotation around the C5–C6 bond, but no transition to the twisted boat conformer. By subtracting the free energy differences related to the various processes, the puckering free energy of the glucose twist boat was estimated to be about 25 kJ/mol<sup>67</sup>. It is worth mentioning, that AFM spectroscopy was first employed to estimate puckering free energies of glucose boats conformers on carboxymethyl amylose (CMA)<sup>68,69</sup>. The reported free energy estimates are in the range 15–18 kJ/mol, therefore quite different from the results obtained from dextran. The estimate obtained from CMA, however, could be biased because of the inability of a freely jointed chain model to fit the force-extension curves of CMA, which prefers a pseudo-helical conformation, as it has been pointed out already in Ref. 66. Recently, Kuttel and Naidoo<sup>70</sup> suggested that in amylose stretching the elongation might be due to a complex rotation of glycosidic linkages, and that chair to boat transitions could play little role in the process.

In the field of computer simulations, ab-initio predictions of the puckering free energy of pyranoses are even more scarce: we are only aware of a Car–Parrinello metadynamics of glucose in vacuum<sup>71</sup> (where, unfortunately, use of non-optimal collective variables has been made of<sup>72</sup>), a Møller-Plesset perturbation approach with inclusion of solvation free energies contributions<sup>73</sup>, and a DFT calculation at the B3LYP/6-311++G\*\* level<sup>74</sup>. A recent, systematic investigation at the B3LYP/6-311++G\*\* level of all epimers of glucose<sup>75</sup> is worth of notice, although only potential energy has been calculated. The calculations of Appell and coworkers<sup>74</sup> predicted a free energy difference for the <sup>1</sup>C<sub>4</sub> conformer of  $\alpha$ -D-Glc and  $\beta$ -D-Glc of 20.40 and 29.18 kJ/mol, respectively. On the contrary, the calculations of Barrows and coworkers<sup>73</sup> suggested a free energy of  $\beta$ -D-Glc <sup>1</sup>C<sub>4</sub> conformer of about 57 kJ/mol. This estimate appears to be substantially higher than all other ones reported so far. In absence of similar ab-initio calculations for idose, that could be employed as benchmark system, it is in our opinion difficult to assess the confidence level of this estimate.

### III. NMR CONFORMATIONAL ANALYSIS OF D-ALTROSE

The semiempirical and molecular mechanical results suggest that an estimate of conformer population by means of NMR spectrometry should be viable also for altrose, which is expected to have a free energy difference lower than 10 kJ/mol. With the aim of determining this free energy difference, we performed the complete assignment of the 400 MHz  $^1\text{H}$  spectrum of altrose in water and methanol solution, also relying on previously published NMR data<sup>64,76,77</sup>, through analysis of the 1D (differential coupling experiments) and 2D (mainly HSQC)-NMR techniques. Gradient enhanced version of the DQF-COSY, TOCSY, HSQC and HMBC techniques were used for signal assignments whereas differential  $^1\text{H}/^1\text{H}$  decoupling, J-resolved spectroscopy and high resolution HSQC measurements were used for establishing the proton J couplings.

The  $^1\text{H}$ -NMR analysis of D-altrose is strongly hindered by the huge overlap among  $^1\text{H}$ -signals of the different structural isomers (pyranose and furanose forms) among which it distributed in aqueous solution. The determination of the  $^3\text{J}_{\text{HH}}$  coupling patterns of the altropyranose, as presented in Tab. II, mainly derive from the high digital resolution ( $4096 \times 1024$  datapoints) HSQC-NMR spectrum.

We have chosen  $\text{J}_{2-3}$  (ax-ax in  $^1\text{C}_4$ ) and  $\text{J}_{4-5}$  (eq-eq in  $^1\text{C}_4$ ) as sensitive probes for the conformational transition. Since we were expecting altrose to exist almost only in  $^4\text{C}_1$  conformation in solvents with lower dielectric permittivity, we have recorded and assigned the spectra also for altrose in deuterated methanol, thus considering its coupling patterns to be representative of the limit forms in water,  $\text{J}(\text{ax}/\text{ax})=9.8$  and  $\text{J}(\text{eq}/\text{eq})=3.6$ . A subsequent metadynamics simulation of altrose in methanol employing the force field presented in this work (Section VIB) showed indeed a dramatic bias towards the  $^4\text{C}_1$  form with respect to the results in water, confirming the trend we expected. Using these values of the coupling constants for the limit forms, the measured  $\text{J}_{2-3}$  and  $\text{J}_{4-5}$  in  $\text{D}_2\text{O}$  appear to be the average from a population of 68 and 65%  $^4\text{C}_1$ , respectively. Thus, our analysis leads to an estimated molar fraction for the  $^4\text{C}_1$  conformer of  $0.66 \pm 0.02$ . The same procedure can be employed to estimate the molar fraction of the puckered conformers of  $\beta$ -D-altrose, assuming an averaged  $\text{J}(\text{eq}/\text{eq}) = 3.6$  Hz for all  $^4\text{C}_1$  conformations and an averaged  $\text{J}(\text{ax}/\text{ax}) = 9.8$  Hz for all  $^1\text{C}_4$  conformations. This leads to an estimated molar fraction of  $0.90 \pm 0.02$  for the  $^4\text{C}_1$  conformer.

It has to be noted that a decade ago, Lichenthaler and coworkers<sup>77-79</sup> found that

$\alpha$ -cycloaltrin could exist as a fast equilibrating mixture of three different conformations ( ${}^4C_1$ ,  ${}^1C_4$  and  ${}^0S_2$ ) in almost the same relative molar ratio. If we apply the Lichtenthaler three states model to the monosaccharide  $\alpha$  altropyranose, the relative population of the  ${}^4C_1$ ,  ${}^0S_2$  and  ${}^1C_4$  would be 62:19:19. Even Snyder and Serianni discussed the possibility of that skew conformation (reported with the alternative name of  ${}^3S_5$ ) being a possible form of  $\alpha$ -D-idose. However, their conclusion was based on the fact that the measured  ${}^3J_{H_4,H_5}$  was not fully compatible with the inverted chair form. In our case, certainly, nothing prevents to employ a three state model but, differently from the case of idose, there is also no explicit need to introduce a population of skwes to interpret the averaged coupling constants.

By inverting Boltzmann formula under the two-states assumption, one can estimate the free energy of the inverted chair to be  $1.6\pm 0.2$  and  $5.5\pm 0.5$  kJ/mol for  $\alpha$  and  $\beta$ -D-altrose, respectively. The theoretical estimates of Angyal<sup>61</sup> (0.8 and 8.4 kJ/mol) and of Vijayalakshmi and Rao<sup>62</sup> (4.4 and 8.9 kJ/mol ) are thus in agreement with our measured values within roughly 3 kJ/mol. By and large, these results on altrose confirm that the estimates of Refs. 61 and 62 represent reasonable approximations of pyranoses free energy difference between chair conformers. Thus, in this work we will use these theoretical estimates as a reference when testing new force field parameter sets.

## IV. COMPUTATIONAL METHODS

### A. Refining Metadynamics with Umbrella Sampling

The term metadynamics identifies a number of techniques that have been devised during the last decade to accelerate dynamics for systems displaying meta-stabilities (see for example Refs. 80–83). All these variants share the usage of a time-dependent biasing potential,  $U_{\text{bias}}[s(x), t]$ , to ease the exploration of the phase space along suitably chosen collective variables,  $s(x)$ , in turn themselves functions of the atomic coordinates  $x$ . The collective variables must represent all slow degrees of freedom characterizing the system, in order for metadynamics – as well as any other free energy profile reconstruction method – to be meaningful<sup>84</sup>.

The direct metadynamics approach<sup>82</sup> shares many traits with other enhanced sampling methods, such as the Local Elevation method<sup>85</sup> or the adaptive umbrella sampling<sup>86</sup> (detailed

lists of enhanced sampling techniques based on molecular dynamics can be found in Refs. 43 and 84), but the fact that the free energy landscape in metadynamics is usually estimated as the negative of the biasing potential in a single, out-of-equilibrium sweep, makes the technique susceptible, at least in principle, of errors introduced by the deposition protocol. Distinct approaches have been devised to estimate the statistical and systematic errors in metadynamics, and also to recover a truly equilibrium free energy profile<sup>51,82,87</sup>. Among these, the approach proposed by Babin and coworkers<sup>51</sup> is in our opinion one of the most intuitive and versatile ones, since it allows in a simple way to simultaneously estimate the statistical error and to eliminate systematic errors introduced by the deposition protocol. The basic idea is the following: a metadynamics run is performed up to the build-up time  $t_b$ , so that the whole collective variables space has been explored, and the total potential energy – sum of the physical and the bias potential – at the end of the run reads

$$V(x) = U(x) + U_{\text{bias}}[s(x), t_b] \quad . \quad (1)$$

At this point, a molecular dynamics simulation in the potential  $V$  is performed, much in the spirit of umbrella sampling, whereas the biasing potential has been determined in an adaptive way by the metadynamics run. The dynamics is characterized by an almost diffusive behavior in the collective variables space, since the meta-stabilities have been removed by the bias potential, provided that all the states of the new potential  $V(x)$  are separated by energy barriers comparable or lower than the thermal energy scale  $k_B T$ . The deviation from a truly diffusive behavior is due by residual features of the free energy landscape which are originated from the statistical and systematic errors in the metadynamics run. During this equilibrium run, the phase space is sampled with probability density

$$\rho_{\text{bias}}(s) = \frac{e^{-\beta\{F(s)+U_{\text{bias}}[s(x),t_b]\}}}{\int ds e^{-\beta\{F(s)+U_{\text{bias}}[s(x),t_b]\}}} \quad (2)$$

that can be estimated by computing the histogram  $\rho_{\text{bias}}(s) = (t - t_b)^{-1} \int_{t_b}^t \delta[s - s(t')] dt'$  during the run. Eventually, the free energy profile is given, up to an additive constant, by

$$F(s) = -U_{\text{bias}}[s(x), t_b] - k_B T \ln \rho_{\text{bias}}(s). \quad (3)$$

In the exact expression Eq. 3, the term  $k_B T \ln \rho_{\text{bias}}(s)$  can be regarded as a correction to what is the standard metadynamics estimate of the free energy landscape,  $F_{\text{meta}}(s) = -U_{\text{bias}}(s)$ . This correction term compensates for the systematic errors introduced by the deposition

protocol, which are not completely under control in the metadynamics run. In other words, from a simple metadynamics run there is no way to guarantee that the term  $\rho_{\text{bias}}(s)$  has become a constant within statistical fluctuations. The corresponding statistical error can be estimated from the fluctuations of  $\rho_{\text{bias}}(s)$  using standard error analysis. Differently from the approach involving only a metadynamics run, one should not worry about the speed of the deposition process (which involves the height, width and deposition rate of the Gaussian functions) as long as the subsequent equilibrium run is ergodic. This means that the Gaussian functions placed during the build-up phase have only to (a) be smaller than  $k_{\text{B}}T$ , (b) being of width comparable or smaller than the finest detail of the free energy landscape which is *deeper* than  $k_{\text{B}}T$  and (c) cover the whole conformational space of the collective variables.

This idea of employing the biasing potential with an umbrella-like sampling has been applied, besides to metadynamics<sup>51</sup>, also to the local elevation method<sup>43</sup>.

## B. Puckering Coordinates

The generalized coordinates introduced by Cremer and Pople<sup>52,53</sup> can be used to identify puckered conformations of rings with an arbitrary number of members. Their definition makes use of the projections  $z_j$  of the position vector of each ring atom onto the normal of the mean ring plane. In the case of six-membered rings the Cremer-Pople coordinates can be defined in terms of the distances  $z_j$  as a functions of 3 parameters  $q_2$ ,  $\phi_2$  and  $q_3$ ), by

$$q_2 \cos \phi_2 = \sqrt{\frac{1}{3}} \sum_{j=1}^6 z_j \cos \left[ \frac{2\pi}{3}(j-1) \right] \quad (4)$$

$$q_2 \sin \phi_2 = -\sqrt{\frac{1}{3}} \sum_{j=1}^6 z_j \sin \left[ \frac{2\pi}{3}(j-1) \right] \quad (5)$$

$$q_3 = \sqrt{\frac{1}{6}} \sum_{j=1}^6 (-1)^{j-1} z_j \quad . \quad (6)$$

This coordinate set  $(q_2, \phi_2, q_3)$  can be conveniently expressed as a spherical coordinate set  $(Q, \theta, \phi)$ ,

$$\begin{cases} q_2 \cos \phi_2 = Q \sin \theta \cos \phi \\ q_2 \sin \phi_2 = Q \sin \theta \sin \phi \\ q_3 = Q \cos \theta, \end{cases} \quad (7)$$

where  $\theta \in [0, \pi]$ ,  $\phi \in [0, 2\pi)$  and  $Q$ , the so-called total puckering amplitude, is defined as  $Q^2 \equiv \sum_{j=1}^N z_j^2 = \sum_m q_m^2$ .

There are two main interconversion paths in pyranoses, namely, the inversion path — connecting the  ${}^4C_1$  and  ${}^1C_4$  conformers — and the pseudo-rotation path<sup>52</sup> — connecting the more flexible boat and skew-boat conformers — that can be easily represented in this coordinate set. The inversion path develops along the  $\theta$  coordinate from the  ${}^4C_1$  conformer at  $\theta = 0$  to the  ${}^1C_4$  one at  $\theta = \pi$ , while the pseudo-rotation one develops along  $\phi$ , at  $\theta = \pi/2$ . Notice that  $\phi$  is a  $2\pi$ -periodic coordinate, meaning that points at  $\phi = 0$  or  $\phi = 2\pi$  (at a given value of  $\theta$ ) represent the same conformer. This is not true for  $\theta$ , which is not periodic.

In this sense, the spherical set  $(Q, \theta, \phi)$  has the advantage that only the two angular variables are needed as collective variables in order to perform a proper — that is, ergodic and unbiased — exploration of the puckered conformations space of typical six-membered rings. This is because along the radial direction no meta-stabilities occur, and the radial coordinate  $Q$  relaxes fast enough to be ergodic for every reasonable set of potential (that is, when the bond lengths are rigid or quasi-rigid). As we showed in a previous work<sup>72</sup>, not every representation of the Cremer–Pople coordinates is equivalent to the end of being used as collective variables for a conformational search. In particular, any two-dimensional subset of Cremer–Pople coordinates whose functional form involves also biasing forces along the direction of  $Q$  might suffer from lack of ergodicity and, therefore, lead to biased sampling<sup>84</sup>. In this work we make only use of the angular variables of the spherical coordinate set as collective variables for the metadynamics run.

Alternative generalized coordinates can be in principle employed to characterize the puckered conformers of six-membered rings, such as the three out-of-plane dihedrals introduced by Strauss and Pickett<sup>88</sup>, or other definitions based on three internal dihedral angles<sup>89–91</sup>. All these alternative schemes produce good puckering coordinates, in the sense that they allow to uniquely map the complete puckering conformational space. However, in the context of conformational search using accelerated methods, oppositely to Cremer–Pople coordinates, (a) they require the exploration of the complete three-dimensional space, being therefore less convenient than a two dimensional phase space search, and (b) the set of micro-states corresponding to the different conformers generally define less simple surfaces which, as it will be discussed later, might affect the determination of the relative populations of conformers.

### C. Simulation Details

The metadynamics and equilibrium simulations have been performed using a version of the GROMETA simulation package<sup>92–95</sup>, previously modified to allow the usage of the  $\theta$  and  $\phi$  angular coordinates of Cremer and Pople, as described in Ref. 72. For each of the 16 D-aldopyranoses, a system composed of the respective sugar ring in a cubic simulation box filled with 504 water molecule was set up. The SPC<sup>96</sup> model has been used to describe the water molecules employed to solvate each of the pyranoses. The SETTLE algorithm has been used to make water rigid<sup>97</sup>, and all bond lengths in the sugar molecules have been constrained using the SHAKE algorithm<sup>98</sup>. An integration step of 0.2 fs has been used for every phase of the simulations. Before starting each run, a 100 ps long molecular dynamics simulation with no bias has been performed to equilibrate the different sugars in their <sup>4</sup>C<sub>1</sub> conformer.

The metadynamics part of the run consisted in a 4 ns long simulation, using Gaussian potential functions of height 0.5 kJ/mol and with 0.05 rad for both angular variables, to build up the biasing potential. Gaussian functions have been placed every 200 integration steps. The Nosé–Hoover<sup>99,100</sup> thermostat and the Parrinello–Rahman<sup>101</sup> barostat have been applied to simulate isothermal-isobaric conditions at 300 K and 1 atm using relaxation times of 0.1 and 1.0 ps, respectively. The simulation box edges have been kept orthogonal, and have been rescaled using an isotropic pressure coupling, which controlled the trace of the pressure tensor.

Each metadynamics run has been then followed by a 4 ns long equilibrium molecular dynamics run at the same thermodynamic conditions, using the set of Gaussians placed during the metadynamics to generate the time-independent biasing potential. At a difference with Ref. 51, where the Lagrangian metadynamics with truncated Gaussians has been employed, we make use of the standard direct metadynamics. During this run, the histogram  $\rho_{\text{bias}}(\theta, \phi)$  has been collected by sampling configurations every 40 fs on a grid of  $60 \times 60$  points.

### V. PUCKERING FREE ENERGY OF GLUCOSE

The combined metadynamics–umbrella sampling has been first applied to the calculation of the puckering free energy profile of  $\beta$ -D-Glc, employing the standard GROMOS 45a4 pa-

parameter set<sup>35</sup>. In Fig. 3 we present the free energy profile as a function of the Cremer–Pople angular variables  $\theta$  and  $\phi$ , showing isolines separated by 10 kJ/mol (upper panel). In order to facilitate the comprehension of the plot, the projection of the free energy profile onto the  $\phi = 0$  plane (lower panel) is also provided: the lower contour of the colored region in the projected profile allows to easily identify the minima along the  $\theta$  coordinate (the minima of this lower contour) and the transition states, or free energy saddle points (the maxima of the lower contour). On the  $(\theta, \phi)$  plane,  ${}^4\text{C}_1$  (0,-),  ${}^1\text{C}_4$  ( $\pi$ ,-), and  ${}^3,{}^{\text{O}}\text{B}$  ( $\pi/2,0$ ) conformers are clearly recognizable as minima basins. Notice that, due to the periodic nature of  $\phi$ , the  ${}^3,{}^{\text{O}}\text{B}$  conformer appears in this representation to be split in two across the  $\phi = 0$  line. Another local minimum basin, more shallow than the previous ones is located around the  ${}^1\text{S}_3$  ( $\pi/2,7\pi/6$ ) conformer and seems to include also some other near boat-like conformer. This kind of occurrence can be a natural feature for gluco-pyranoses, because of the high flexibility of the ring conformers along the pseudo-rotational path (located at  $\theta = \pi/2$ ). A more detailed description of this local minimum is anyway beyond the interest of this work, because of its very high free energy.

In addition to the free energy profile, in Fig. 4 we show an analogous plot, presented both on the  $(\theta, \phi)$  plane (upper panel), and projected onto the  $\phi = 0$  plane (lower panel), of the correction to the free energy profile coming from the umbrella sampling phase,  $-k_{\text{B}}T \ln \rho_{\text{bias}}(s)$ . Performing a screening of this contribution is quite important, because it allows to check if residual meta-stabilities (recognizable as basins) are left after the metadynamics phase, and whether an ergodic sample of the interesting region in the  $(\theta, \phi)$  plane has been performed or not: poorly sampled regions will appear as peaks. In Fig. 4 it is possible to see that the metadynamics run performed reasonably well. Indeed, the paths connecting the original metastable states do not show residual metastabilities. It is seen that the complete space of puckering angles has been sampled properly. Corrections to the free energy difference between  ${}^4\text{C}_1$  and  ${}^1\text{C}_4$  are  $\simeq 2$  kJ/mol. In case of the next most populated state,  ${}^3,{}^{\text{O}}\text{B}$ , the correction increases to  $\simeq 4$  kJ/mol, while for other states the correction can reach, but never exceeds,  $\simeq 6$  kJ/mol with respect to the free energy of  ${}^4\text{C}_1$ . The umbrella phase thus contributes in a significant way to the estimate of free energy differences, and — as expected — appears to be more important for less populated states and for transition states.

Both the  ${}^1\text{C}_4$  and  ${}^3,{}^{\text{O}}\text{B}$  puckering free energies (local minima at about 10 and 17 kJ/mol, respectively) appear to be lower than what one would expect. In particular, the free energy

of the inverted chair is about 15 kJ/mol lower than both our reference values<sup>61,62</sup>. This free energy difference leads to a inverted chair population of about 1%, which can be observed during regular molecular dynamics runs at equilibrium. While not strictly incompatible with NMR experiments, which usually can predict populations with a  $\simeq 2\%$  accuracy, this value is certainly strikingly lower than all other theoretical estimates. This fact is even more important if one considers that  $\beta$ -D-Glc is supposed to have the largest  ${}^1C_4$  free energy among aldopyranoses. It is thus expected that the  ${}^1C_4$  conformers of the other stereoisomers could be characterized by even lower free energy differences. As it will be discussed in Sec.VI, this scenario is only partially correct, as unexpected patterns of the chair–inverted chair free energy difference appear along the series.

A more direct connection with experimentally measurable quantities is performed through the calculation of the population of the basins associated with each of the recognizable conformers. To this aim, the  $(\theta, \phi)$  plane has been partitioned in four regions covering the four main basins:  $\theta \in [0, \pi/3]$ , associated to  ${}^4C_1$ ;  $\theta \in [2\pi/3, \pi]$ , associated to  ${}^1C_4$ ;  $\theta \in [\pi/3, 2\pi/3]$  and  $\phi \in [-2\pi/3, 2\pi/3]$ , associated to  ${}^3,0B$ ;  $\theta \in [\pi/3, 2\pi/3]$  and  $\phi \in [2\pi/3, 4\pi/3]$ , associated to the mixture around  ${}^1S_3$ . This partitioning of the conformational space appears to be quite natural, since the separating lines are located with good approximation along the maxima of the free energy surface (as is evident especially from the side-view of the free energy landscape, lower panel of Fig. 3) and, therefore, also close to the transition states. The population of a region  $\Omega$  can then be calculated simply as

$$p(\Omega) = Z^{-1} \int_{\Omega} e^{-F(\theta,\phi)/k_B T} d\theta d\phi \quad (8)$$

where the integral of the normalization factor

$$Z = \int e^{-F(\theta,\phi)/k_B T} d\theta d\phi \quad (9)$$

is extended to the whole  $(\theta, \phi)$  space. According to this numerical estimate, the  ${}^4C_1, {}^1C_4, {}^3,0B$  and  ${}^1S_3$  conformations account for 98.42, 1.52, 0.0461 and  $3.7 \times 10^{-4}\%$  of the total population, respectively.

When the manuscript was in preparation, we discovered that Hansen and Hüneneberger already performed an analysis of the puckering free energy of glucose<sup>43</sup>. To our surprise, their estimates of the inverted chair free energy differ by a non-negligible amount from that presented here, although the same force field and thermodynamic conditions have been used.

In the approach of Hansen and Hünenberger, free energies are derived from populations by inverting Boltzmann formula. We did the same and obtained a value of 10.43 kJ/mol for the free energy of  ${}^1C_4$ , while in Ref. 43 this value ranged from 16.0 to 16.5 kJ/mol (see Tab.4 in Ref.<sup>43</sup>) The difference between these two approaches is quite important, as it translates to inverted chair populations of  $\simeq 1\%$  and  $\simeq 0.1\%$  for the results of this work and of Ref.43, respectively. Notice that in a recent work Spiwok and coworkers found the  ${}^1C_4$  free energy of  $\beta$ -D-Glc to be  $11.6\pm 1.8$  (thus, compatible with our findings) using the 45a4 force field and a metadynamics employing all three Cremer-Pople coordinates as collective variables.

We give here a tentative explanation of the difference with the results of Ref. 43. The difference is most probably not related to which set of collective variables (Pickett dihedrals versus Cremer–Pople coordinates) has been used to enhance the sampling, because both sets of coordinates represent every slow degree of freedom and allow to span the three-dimensional puckering conformational space in an ergodic way. Systematic errors related to the accelerated dynamics should have been eliminated in both approaches, since both sampling methods provide an unbiased estimate, thanks to the equilibrium sampling. Hence, among the possible reasons left are: the use of different algorithms for the simulation of isothermal–isobaric conditions; the different system size; cut-off and long range corrections. Another explanation could be the way different states are defined: partitioning a three dimensional conformational space is far more complicated than partitioning a two dimensional space. In the former case identifying in a proper way the different basins might lead to a miscounting of states, while in the latter one only straight cuts along the  $\theta$  and  $\phi$  directions are needed. Still, more investigation would be needed to address properly this subject, which is out of the scope of this work.

## VI. PUCKERING FREE ENERGY OF ALDOPYRANOSSES

### A. The 45a4 Parameter Set

Apart from the problems related to a correct definition of different puckered states, it is clear that the calculation of the free energy profile of  $\beta$ -D-Glc alone cannot be considered exhaustive nor satisfactorily. The theoretical estimates predict a great variety in the conformational free energies of the 16 stereoisomers of  $\beta$ -D-Glc, and puckering properties have to be

checked separately for each of them. For these reasons we decided to compute in a systematic way the puckering free energy landscape for the whole series of  $\alpha$  and  $\beta$ -D-pyranoses.

From the point of view of the force field, the stereoisomers of glucose differ only slightly, namely (a) the order of the two central atoms involved in an improper dihedral interaction at a chiral centre has to be inverted, in order to move a residue from the equatorial to the axial conformation; (b)  $\alpha$  anomers are distinguished from  $\beta$  anomers by different torsional interactions on the O5–C1–O1–H1 dihedral, and (c) those sugars having O4 and C6 located on the same side of the ring plane (galactose, talose, gulose, idose) are modeled with different parameters for the O5–C5–C6–O6 and C4–C5–C6–O6 dihedral angles<sup>35</sup>.

Simulations of the remaining 15 stereoisomers of glucose have been performed using the same protocol employed for  $\beta$ -D-Glc. We summarized the results in Fig. 5 and Tab. III. In Fig. 5 we report the free energy difference between the  ${}^1C_4$  and  ${}^4C_1$  conformers of  $\alpha$  and  $\beta$ -D-pyranoses modeled using the 45a4 force field, along with the theoretical estimates of Angyal<sup>61</sup> and of Vijayalakshmi and coworkers<sup>62</sup>. Two horizontal dashed lines are also drawn at 0 and 5 kJ/mol (approximately  $2k_B T$  at room temperature), highlighting the thresholds below which the inverted chair population becomes greater than the chair one, and below which the inverted chair population becomes noticeable, respectively. In Tab. III, free energy differences and populations for the complete  $\alpha$  and  $\beta$  series are listed. The free energy difference and population of the next leading conformer (after  ${}^1C_4$ ) are also reported, as well as the location on the  $(\theta, \phi)$  plane of the first transitions next to  ${}^4C_1$ . Concerning the population of the leading next conformer, the values reported were calculated on the  $\theta \in [\pi/3, 2\pi/3]$  region. This choice takes into account all other local minima present along the equatorial line, but their free energy is always so large (as it has been seen for  $\beta$ -D-Glc), that this approximation does not change substantially the population of the next leading conformer.

The differences between the theoretical estimates and the simulation results obtained using the GROMOS 45a4 force field are striking. First of all, none of the 16 sugars investigated presents a chair/inverted chair free energy difference in quantitative agreement with the theory, as differences are usually larger than 5 kJ/mol, and in many cases even larger than 10 kJ/mol. More importantly, many of these values are in marked qualitative disagreement not only with the theoretical results, but also with experimental evidence. In fact,  $\alpha$ -D-Glc,  $\alpha$ -D-Gal,  $\alpha$ -D-Man,  $\beta$ -D-Gal and  $\beta$ -D-Man present an inverted chair free energy which is

lower than  $2 k_B T$  at room temperature. This means that a sensible population of inverted chairs, of the order of 10% is expected at equilibrium, in contrast with no experimental evidence of the occurrence of this conformer. The same behavior is even more pronounced in D-Tal, displaying an inverted chair free energy close to zero. On the contrary, the puckering free energy of idose inverted chairs simulated using the 45a4 set of parameters results to be greater than 10 kJ/mol, therefore ruling out the possibility of observing idose inverted chairs in equilibrium simulations.

The GROMOS 45a4 force field appears to be unable not only to compare quantitatively with experimental and theoretical results, but — even more importantly — to reproduce the qualitative behavior of any of the two series. Given the ubiquitous presence of galactose and mannose in relevant oligo and polysaccharides of biological origin, the inability of the force field to prevent appearance of inverted chairs at room temperature seems to be a severe drawback, at least for out-of-equilibrium simulations.

While the free energy of different ring conformers is certainly an important physical quantity, one should not overlook the importance of the kinetics of the conformational transitions. One might reason that alternate conformers might not be seen during equilibrium simulations, if the inverse transition rate is much longer than the typical time interval spanned by a simulation. This pragmatic approach could be hazardous, given the fast pace of increase in simulations sizes and lengths, but nevertheless appealing. Kräutler and coworkers<sup>28</sup> reported that in 200 ns long simulation runs of  $\beta$ -D-Glc,  $\beta$ -D-Gal,  $\beta$ -D-Man and  $\beta$ -D-Tal, all sugars but glucose remained for more than 99.9% of the time in the chair conformation, while glucose was found in boat and twisted conformation for the 0.7% of the time (giving a rough estimate of the characteristic time of escape from the chair conformer basin of 10 ns).

Although 200 ns is a time much longer than that of most simulations, one should keep in mind that conformational transitions are stochastic events, and a characteristic time of 10 ns might lead to a considerable amount of “unwanted” conformers in simulation runs much shorter than 200 ns, but with more than just one sugar molecule in solution. We tested a setting which we consider to be representative of a typical simulation of medium to large size, namely, of a 25 ns long run at constant temperature and pressure of 512  $\beta$ -D-Glc and  $25 \times 10^3$  water molecules in a simulation box with an edge of approximately 9.6 nm, using a cut-off of 1.3 nm for every nonbonded interaction, and an integration timestep of 2 fs.

Every other parameter and algorithm employed has been the same as in the metadynamics run discussed so far. Indeed, we observed the appearance of both boats and inverted chairs conformers, with a statistical frequency of 0.06% and 1.1%, respectively (see the upper panel of Fig. 6. These values are close to the one expected from the free energy calculations (see Tab. III). However, a look at the time evolution of the number of inverted chair in the simulation box (lower panel of Fig. 6) tells us that equilibrium has not been reached yet. Still, this result is to our opinion quite valuable, because it gives some information about the kinetics of ring conformational transitions in  $\beta$ -D-Glc, showing that it is not unlikely to observe inverted chair conformers in equilibrium simulations of conventional size, using the 45a4 parameter set.

We performed similar simulations of other sugars, namely,  $\beta$ -D-Gal and  $\alpha$ -D-Glc, and in both cases we observed the appearance of inverted chairs, although to a much smaller extent, showing that the kinetics of the chair to inverted chair transition is much slower in these cases (consistently with the results of Ref. 28). This fact is obviously related to the height of the barrier that separates  ${}^4C_1$  conformers from other ones (see Tab. III), which appears to be lower in  $\beta$ -D-Glc than in all other cases.

## B. Force Field Re-parametrization

After realizing the difficulties of the 45a4 parameter set in reproducing puckering properties of pyranoses, we planned to re-parametrize the force field, by finding a minimal set of changes that could fix at least the qualitative aspects discussed so far. At a first glance, this task could seem a bit intimidating, because puckering variables (and therefore the relative free energy landscapes) depend directly on all six ring atoms and also — indirectly, but possibly to a considerable extent — on the ring substituents. The number of parameters on which puckering free energy depends is, therefore, quite high. A completely automated procedure is out of question, and one needs to adopt an heuristic approach.

To keep the re-parametrization as general as possible, and the number of parameters to be tuned low, we decided that our approach should adhere to the following criteria: (a) only parameters not directly involved in inter-molecular interactions should be tuned; (b) the changes should not be sugar-dependent; (c) the changes have to preserve previously known or already tuned molecular properties; (d) the inverted chair free energy of most common

sugars (glucose, galactose, mannose) should be higher than 10 kJ/mol; (e) the trend of the inverted chair free energy as a function of the sugar type, as well as (f) the approximate offset between the inverted chair free energies of  $\alpha$  and  $\beta$  anomers, have to be reproduced.

Within this framework, a complete, quantitative agreement for every sugar type is most probably not feasible, especially given the constraints (a) and (b). However, we found that quite reasonable results can be indeed achieved with minimal parameter changes. Point (a) requires Lennard-Jones parameters and partial charges of the 45a4 parameter set to be preserved. Together with the requirement at point (d), this suggests that only angular or torsional interactions involving three or more ring atoms should be the target of our optimization. This is because among the known properties which are well reproduced by the GROMOS 45a4 force field there are the rotameric distribution of the hydroxymethyl group and the conformation of the glycosidic linkages (in di-saccharides). We realized quite soon that changing the stiffness of angular interactions did not change the puckering free energy noticeably. Spieser and coworkers<sup>34</sup> showed that the height of the energetic barrier between  ${}^4C_1$  and  ${}^1C_4$  can be increased by stiffening the angular interactions. However, this affects only the free energy of the transition states, and not the free energy difference of the metastable conformers.

Therefore, we concentrated on the torsional interactions, and noticed that every torsional interaction involving three ring atoms (C1,C2,C3,C4,C5 or O5) and either C6 or any hydroxyl oxygen (O1,O2,O3,O4) was either not present (this is the case of O4-C4-C5-O5, C3-C4-C5-C6, O2-C2-C1-O5, C1-O5-C5-C6 and C5-O5-C1-O1) or present with a phase term  $\cos(\delta) = +1$  and multiplicity  $n = 2$  in the torsional potential

$$U(\phi) = k_\phi [1 + \cos(\delta) \cos(n\phi)], \quad (10)$$

associated to the dihedral angle  $\phi$ . As it was pointed out in Ref. 43, such a phase favors the axial conformation of the substituent, with respect to the equatorial one, whereas a negative value of  $\cos(\delta)$  would favor the equatorial conformation with respect to the axial one. Indeed, one of those interactions (O2-C2-C1-O5) has been eliminated in the 45a4 version of the GROMOS force field, for the precise purpose of stabilizing the  ${}^4C_1$  conformer. While this is true for glucose, it is not, *e.g.*, for mannose, whose substituent in C2 is axial in the chair conformer. Therefore, the change in the 45a4 set that stabilized the glucose chair, acted in the opposite direction for mannose, stabilizing the inverted chair.

It is clear that any change affecting these torsional parameters will have a profound (and sugar-specific) effect on the whole series of pyranoses. Therefore, to make grounded changes to the force field, one has first to understand how the pattern of axial and equatorial substituent in the  ${}^4C_1$  conformer, for given torsional interactions involving the five chiral centres, can influence the properties of the  ${}^1C_4$  free energy curves of the  $\alpha$  and  $\beta$  series.

Firstly, we realized that by changing the sign of  $\cos(\delta)$  in the C1–C2–C3–O3 and C5–C4–C3–O3 interactions, one can at the same time rise the  ${}^1C_4$  free energy of glucose, galactose, mannose, and talose, and lower that of allose, gulose, altrose and idose. Looking at the location along the free energy series of these sugars, it appears that these interactions are leading candidates to recover the approximate monotonous trend in the  ${}^1C_4$  free energy and, consequently, to fix consequently point (e).

Another important role in determining the shape of the free energy curve is played by a dihedral interaction which is not present in the 45a4 parameter set, namely, the one involving the substituent at the C5 chiral center. The chirality of C5 is the same for all 16 stereoisomers of D-Glc, and can be actually exploited to introduce a global shift for the  ${}^1C_4$  free energies of the whole series of 16 D-pyranoses. While this gives some freedom in our parametrization process, it should be kept in mind that, most probably, parameters optimized this way are not valid to model the series of L-pyranoses.

In addition to the interactions discussed so far, to reproduce correctly the gap between the  ${}^1C_4$  free energy curves of the  $\alpha$  and  $\beta$  series — as it is apparent, for example, in the theoretical data presented in Fig. 5 — the torsional interaction for the C3–C2–C1–O1 present in the 45a4 set has to be modified. The chirality of the C1 carbon atom differs only between the  $\alpha$  and  $\beta$  anomers, and is certainly playing a role in modulating the height of the free energy gap between  $\alpha$  and  $\beta$  anomers.

Eventually, corrections to the energy term associated to the dihedral C4–C3–C2–O2 were proven to enhance the agreement to the theoretical estimates.

In summary, the phase and amplitude of the C3–C2–C1–O1, C4–C3–C2–O2, C1–C2–C3–O3, C5–C4–C3–O3 and C1–O5–C5–C6 torsional interaction were tuned by trial and errors in order to obtain  ${}^1C_4$  free energy curves in better agreement with experimental and theoretical data. The set of torsional interactions and their parameters for the proposed modification to the 45a4 parameter set are reported in Tab. IV, and the full gromacs topologies are provided at <http://www.science.unitn.it/~sega/sugars.html> It is worth mentioning

that the strength of the C1–C2–C3–O3 and C5–C4–C3–O3 torsional interactions had to be set to a much higher value (2.4 kJ/mol) than that of the other ones involving three ring atoms and one hydroxyl oxygen. Given the similar chemical nature of the quadruplets of atoms involved (beside that of the anomeric oxygen), such asymmetry appears to be peculiar. This might originate either from the fact that the O3 oxygen can be involved in the 1,3-trans-diaxial interaction with the hydroxymethyl group (stronger than that with any other OH groups) or from other interaction terms already present in the 45a4 set, whose influence on the puckering free energy is not yet understood, and that might deserve a separate investigation.

The new parametrization of the GROMOS force field for sugars was performed with the aim not to change properties other than puckering, and dihedral interactions directly involved in the rotameric distribution of the hydroxymethyl group were thus not changed. This choice alone, however, is no guarantee that this quantity is not affected. We checked explicitly that these modifications did not affect the rotameric distribution of the hydroxymethyl group, calculating the free energy profile of the C4–C5–C6–O6 torsional angle ( $\omega$ ) for the 45a4 and new sets of parameters. The results obtained with the two parameter sets did not differ more than 2% between each other. The free energy surfaces have been calculated using the same metadynamics/umbrella sampling approach employed for the calculation of the puckering free energy, but using a Gaussian width of 0.1 rad for biasing the  $\omega$  variable.

We summarized the results obtained using our modified set of parameters in Figs. 7,8,9 and Tab. V. In Fig. 7 the free energy differences between inverted chair and chair conformers are compared again with the theoretical predictions of Ref. 62 and Ref. 61. The improvement with respect to the results obtained with the 45a4 set (Fig. 5) is striking. Both the  $\alpha$  and  $\beta$  series reproduce now the qualitative trend of the theoretical estimates. Galactose, mannose, and talose are not anymore below the  $2k_B T$  threshold, and the value of gulose, altrose and idose free energies diminished considerably. Also the gap between the  $\alpha$  and  $\beta$  anomers is now reproduced reasonably well, being on average  $\simeq 5$ kJ/mol. Noticeably, the height of the free energy barrier of  $\beta$ -D-Glc has been increased considerably, from  $\simeq 25$ kJ/mol to  $\simeq 45$ kJ/mol. This increase, which changes dramatically the kinetics of the conformational transition of  $\beta$ -D-Glc, has no counterpart in any other  $\beta$ -anomer. The situation for  $\alpha$ -anomers is slightly different, because the height of the free energy barrier close to  ${}^4C_1$  increased markedly for  $\alpha$ -D-Tal and  $\alpha$ -D-Gul and, at the same time, decreased for  $\alpha$ -D-All and  $\alpha$ -D-Alt. Unfortunately,

the population of inverted chairs in  $\alpha$ -D-Ido is still lower than that of chairs, whereas both theory and experiment show a preference for the  ${}^1C_4$  conformer. However, given the fact that these changes are not sugar-specific, the result obtained is to our opinion still remarkable, as the ability to reproduce puckering properties has increased dramatically, with respect to the 45a4 set.

## VII. CONCLUSIONS

We addressed the problem of the proper modelling of pyranoses puckering properties using the GROMOS force field. A serious problem in such a task is the lack of experimental information on the conformer populations of stereoisomers of glucose other than idose. To fill this gap, we performed the first measurement of altrose chair conformers population by assigning the complete coupling pattern of its  ${}^1H$  NMR spectrum. The estimated populations are in agreement within roughly 5 kJ/mol with available theoretical analyses based on semiempirical and molecular mechanical models, thus confirming their reliability. The theoretical estimates have been therefore employed as target values for the subsequent reparametrization of the force field, for sugars other than idose and altrose.

The realism in reproducing the population of inverted chairs of pyranoses modeled using the 45a4 parameter set of the Gromos force field leaves much to be desired: galactose, mannose, allose, and  $\alpha$ -D-Glc present a sizable population of the inverted chair conformer, while the population of the inverted chair conformer of idose resulted to be negligible in simulation, contrarily to experimental evidence.

We devised a new set of parameters which has proven to be quite successful in recovering the trend of the inverted chair free energy for all 16 stereoisomers under study. Our parametrization reproduces free energy differences in accordance with experimental and theoretical data always within 5 kJ/mol, but in most cases within 2.5 kJ/mol, that is,  $1k_B T$ . A closer agreement with the theoretical models is probably not needed, given the uncertainties to which they are subjected. Indeed, while the theoretical models do not provide any confidence interval, an approximate picture can be obtained by comparing them with the experimental data on idose<sup>50</sup> and altrose (this work), which roughly fall within a 3 kJ/mol interval.

The improvement attained with the introduction of this new parameter set is to our opin-

ion substantial, and reached the goal of reproducing known puckering free energy differences while keeping other properties, such as inter-molecular interactions and the rotameric distribution of the hydroxymethyl group, unchanged. These modifications to the GROMOS force field will allow to perform more realistic simulations of D-aldopyranoses. They represent a certain improvement in the study of carbohydrate equilibrium properties, but will have an even more important impact on the evaluation of out-of-equilibrium properties, such as in the case of simulated AFM pulling experiments.

Still, much has to be done regarding the puckering properties of carbohydrates. In particular, the role of skew conformations — possibly detected in NMR experiments<sup>50,78</sup> but not significantly present in both the 45a4 and new parameter sets — has to be clarified. Other pyranosides and furanoses should also be investigated to further test the force field. The GROMOS force field, however, is not the only one which has been found to be problematic in reproducing proper puckering properties, and for many force fields the investigations of ring conformer populations are scarce, if not missing at all. Our hope is that, beside the usefulness related to the specific case of the GROMOS force field parametrization, this work could also serve to attract attention to the importance of the puckering problem in carbohydrate simulations, and to stimulate further investigations.

### Acknowledgements

The authors thank E. Chiessi for enlightening discussions, and acknowledge the use of the Wiglaf computer cluster of the Department of Physics of the University of Trento. This work has been partially supported by a PRIN grant from the Italian Ministry of Public Education, University and Scientific Research.

---

\* Electronic address: [sega@science.unitn.it](mailto:sega@science.unitn.it)

<sup>1</sup> B. Hardy and A. Sarko, *J. Comput. Chem.* **14**, 848 (1993).

<sup>2</sup> B. Hardy and A. Sarko, *Polymer* **37**, 1833 (1996).

<sup>3</sup> A. Almond, A. Brass, and J. Sheehan, *J. Mol. Biol.* **284**, 1425 (1998).

<sup>4</sup> K. Ueda, A. Imamura, and J. Brady, *J. Phys. Chem. A* **102**, 2749 (1998).

<sup>5</sup> P. Venkatarangan and A. Hopfinger, *J. Med. Chem.* **42**, 2169 (1999).

- <sup>6</sup> K. Lee, D. Benson, and K. Kuczera, *Biochemistry* **39**, 13737 (2000).
- <sup>7</sup> F. Cavalieri, E. Chiessi, M. Paci, G. Paradossi, A. Flaibani, and A. Cesaro, *Macromolecules* **34**, 99 (2001).
- <sup>8</sup> K. Naidoo and M. Kuttel, *J. Comput. Chem.* **22**, 445 (2001).
- <sup>9</sup> Y. W. Kim and W. Sung, *Phy. Rev. E* **63**, 041910 (2001).
- <sup>10</sup> F. Momany and J. Willett, *Biopolymers* **63**, 99 (2002).
- <sup>11</sup> G. Paradossi, F. Cavalieri, and E. Chiessi, *Macromolecules* **35**, 6404 (2002).
- <sup>12</sup> G. Paradossi, E. Chiessi, A. Barbiroli, and D. Fessas, *Biomacromolecules* **3**, 498 (2002).
- <sup>13</sup> L. Lawtrakul, H. Viernstein, and P. Wolschann, *Int. J. Pharm.* **256**, 33 (2003).
- <sup>14</sup> M. Umemura, Y. Yuguchi, and T. Hirotsu, *J. Phys. Chem. A* **108**, 7063 (2004).
- <sup>15</sup> H. Verli and J. Guimarães, *Carbohydr. Res.* **339**, 281 (2004).
- <sup>16</sup> H. Yu, M. Amann, T. Hansson, J. Köhler, G. Wich, and W. van Gunsteren, *Carbohydr. Res.* **339**, 1697 (2004).
- <sup>17</sup> C. Sandoval, C. Castro, L. Gargallo, D. Radic, and J. Freire, *Polymer* **46**, 10437 (2005).
- <sup>18</sup> Y. Xie and A. Soh, *Mater. Lett.* **59**, 971 (2005).
- <sup>19</sup> J. González-Outeiriño, R. Kadirvelraj, and R. Woods, *Carbohydr. Res.* **340**, 1007 (2005).
- <sup>20</sup> A. Palleschi, G. Bocchinfuso, T. Coviello, and F. Alhaique, *Carbohydr. Res.* **340**, 2154 (2005).
- <sup>21</sup> I. Neelov, D. Adolf, T. McLeish, and E. Paci, *Biophys. J.* **91**, 3579 (2006).
- <sup>22</sup> T. Mamonova and M. Kurnikova, *J. Phys. Chem. B* **110**, 25091 (2006).
- <sup>23</sup> A. Figueiras, J. Sarraguça, R. Carvalho, A. Pais, and F. Veiga, *Pharm. Res.* **24**, 377 (2007).
- <sup>24</sup> D. Kony, W. Damm, S. Stoll, W. van Gunsteren, and P. Hünenberger, *Biophys. J.* **93**, 442 (2007).
- <sup>25</sup> Y. Yoshida, A. Isogai, and Y. Tsujii, *Cellulose* **15**, 651 (2008).
- <sup>26</sup> M. Almlöf, E. Kristensen, H. Siegbahn, and J. Åqvist, *Biomaterials* **29**, 4463 (2008).
- <sup>27</sup> M. Umemura and Y. Yuguchi, *Cellulose* **16**, 361 (2009).
- <sup>28</sup> V. Kräutler, M. Müller, and P. Hünenberger, *Carbohydr. Res.* **342**, 2097 (2007).
- <sup>29</sup> S. Perez, A. Imberty, S. Engelsen, J. Gruzza, K. Mazeau, J. Jimenez-Barbero, A. Poveda, J. Espinosa, B. van Eyck, G. Johnson, A. D. French, M. L. C. E. Kouwijzer, P. D. J. Grootenuis, A. Bernardi, L. Raimondi, H. Senderowitz, V. Durier, G. Vergoten, and K. Rasmussen, *Carbohydr. Res.* **314**, 141 (1998).

- <sup>30</sup> J. Behler, D. Price, and M. Drew, *Phys. Chem. Chem. Phys.* **3**, 588 (2001).
- <sup>31</sup> F. Corzana, M. Motawia, C. Hervé Du Penhoat, S. Perez, S. Tschampel, R. J. Woods, and S. Engelsen, *J. Comput. Chem.* **25**, 573 (2004).
- <sup>32</sup> L. Kroon-Batenburg, P. Kruiskamp, J. Vliegthart, and J. Kroon, *J. Phys. Chem. B* **101**, 8454 (1997).
- <sup>33</sup> J. W. Brady, *J. Am. Chem. Soc.* **108**, 8153 (1986).
- <sup>34</sup> S. A. H. Spieser, J. A. van Kuik, L. M. J. Kroon-Batenburg, and J. Kroon, *Carbohydr. Res.* **322**, 264 (1999).
- <sup>35</sup> R. Lins and P. Hünenberger, *J. Comput. Chem.* **26**, 1400 (2005).
- <sup>36</sup> E. Chiessi, private communication.
- <sup>37</sup> H. Limbach and J. Ubbink, *Soft Matter* **4**, 1887 (2008).
- <sup>38</sup> J. E. H. Koehler, W. Saenger, and W. F. van Gunsteren, *Eur. Biophys. J.* **15**, 197 (1987).
- <sup>39</sup> W. F. van Gunsteren, S. R. Billeter, A. A. Eising, P. Hünenberger, P. Krüger, A. E. Mark, W. R. P. Scott, and I. G. Tironi, *The GROMOS96 Manual and User Guide*, Zürich, Switzerland, 1996.
- <sup>40</sup> M. L. C. E. Kouwijzer and P. D. J. Grootenhuis, *J. Phys. Chem.* **99**, 13426 (1995).
- <sup>41</sup> K.-H. Ott and B. Meyer, *J. Com. Chem.* **17**, 1068 (1996).
- <sup>42</sup> W. Damm, A. Frontera, J. Tirado-Rives, and W. Jorgensen, *J. Comput. Chem.* **18**, 1955 (1997).
- <sup>43</sup> H. S. Hansen and P. H. Hünenberger, *J. Comput. Chem.* **31**, 1 (2010).
- <sup>44</sup> V. Spiwok, B. Králová, and I. Tvaroska, *Carbohydr. Res.* **345**, 530 (2010).
- <sup>45</sup> G. Lee, W. Nowak, J. Jaroniec, Q. Zhang, and P. Marszalek, *Biophys. J.* **87**, 1456 (2004).
- <sup>46</sup> B. Heymann and H. Grubmüller, *Chem. Phys. Lett.* **305**, 202 (1999).
- <sup>47</sup> W. D. Cornell, P. Cieplak, C. I. Bayly, I. R. Gould, K. M. Merz, D. M. Ferguson, D. C. Spellmeyer, T. Fox, J. W. Caldwell, and P. A. Kollman, *J. Am. Chem. Soc.* **117**, 5179 (1995).
- <sup>48</sup> R. J. Woods, R. A. Dwek, C. J. Edge, and B. Fraserreid, *J. Phys. Chem.* **99**, 3832 (1995).
- <sup>49</sup> R. Eklund and G. Widmalm, *Carbohydr. Res.* **338**, 393 (2003).
- <sup>50</sup> J. Snyder and A. Serianni, *J. Org. Chem.* **51**, 2694 (1986).
- <sup>51</sup> V. Babin, C. Roland, T. A. Darden, and C. Sagui, *J. Chem. Phys.* **125**, 204909 (2006).
- <sup>52</sup> D. Cremer and J. A. Pople, *J. Am. Chem. Soc.* **97**, 1354 (1975).
- <sup>53</sup> D. Cremer, *J. Phys. Chem.* **94**, 5502 (1990).

- <sup>54</sup> A. McNaught, *Adv. Carbohydr. Chem. Biochem.* **52**, 43 (1997).
- <sup>55</sup> S. Rings, *Eur. J. Biochem.* **100**, 295 (1980).
- <sup>56</sup> D. Cremer and K. Szabo, *Ab initio Studies of Six-Membered Rings, Present Status and Future Developments*, in *Methods in Stereochemical Analysis, Conformational Behavior of Six-Membered Rings, Analysis, Dynamics, and Stereoelectronic Effects*, p. 59, VCH Publishers, 1995.
- <sup>57</sup> V. S. R. Rao, P. K. Qasba, P. Balaji, and R. Chandrasekaran, *Conformation of Carbohydrates*, Harwood Academic Publisher, Amsterdam, 1998.
- <sup>58</sup> H. Sachse, *Ber. Dtsch. Chem. Ges.* **23**, 1363 (1890).
- <sup>59</sup> H. Sachse, *Z. Phys. Chem.* **10**, 203 (1892).
- <sup>60</sup> O. L. Sponsler and W. H. Dore, in *Fourth Colloid Symposium Monograph*, p. 174, Chemical Catalog Company, New York, 1926.
- <sup>61</sup> S. Angyal, *Angew. Chem., Int. Ed.* **8**, 157 (1969).
- <sup>62</sup> K. Vijayalakshmi and V. Rao, *Carbohydr. Res.* **22**, 413 (1972).
- <sup>63</sup> D. Barton, *Science* **169**, 539 (1970).
- <sup>64</sup> Y. Zhu, J. Zajicek, and A. Serianni, *J. Org. Chem.* **66**, 6244 (2001).
- <sup>65</sup> F. Franks, P. Lillford, and G. Robinson, *J. Chem. Soc. Faraday. Trans.* **85**, 2417 (1989).
- <sup>66</sup> P. Marszalek, H. Li, A. Oberhauser, and J. Fernandez, *Proc. Natl. Acad. Sci. USA* **99**, 4278 (2002).
- <sup>67</sup> Q. Zhang, G. Lee, and P. Marszalek, *J. Phys.: Condens. Matter* **17**, S1427 (2005).
- <sup>68</sup> P. Marszalek, A. Oberhauser, Y. Pang, and J. Fernandez, *Nature* **396**, 661 (1998).
- <sup>69</sup> H. Li, M. Rief, F. Oesterhelt, H. Gaub, X. Zhang, and J. Shen, *Chem. Phys. Lett.* **305**, 197 (1999).
- <sup>70</sup> M. Kuttel and K. Naidoo, *J. Am. Chem. Soc.* **127**, 12 (2005).
- <sup>71</sup> X. Biarnes, A. Ardevol, A. Planas, C. Rovira, A. Laio, and M. Parrinello, *J. Am. Chem. Soc.* **129**, 10686 (2007).
- <sup>72</sup> M. Sega, E. Autieri, and F. Pederiva, *J. Chem. Phys.* **130**, 225102 (2009).
- <sup>73</sup> S. Barrows, F. Dulles, C. Cramer, A. French, and D. Truhlar, *Carbohydr. Res.* **276**, 219 (1995).
- <sup>74</sup> M. Appell, G. Strati, J. Willett, and F. Momany, *Carbohydr. Res.* **339**, 537 (2004).
- <sup>75</sup> U. Schnupf, J. Willett, and F. Momany, *Carbohydr. Res.* **345**, 503 (2010).

- <sup>76</sup> M. King-Morris and A. Serianni, *J. Am. Chem. Soc.* **109**, 3501 (1987).
- <sup>77</sup> F. Lichtenthaler, U. Kläres, Z. Szirmai, and B. Werner, *Carbohydr. Res.* **305**, 293 (1997).
- <sup>78</sup> S. Immel, K. Fujita, and F. Lichtenthaler, *Chem. Eur. J.* **5**, 3185 (1999).
- <sup>79</sup> Y. Nogami, K. Nasu, T. Koga, K. Ohta, K. Fujita, S. I. and H. J. Lindner, G. E. Schmitt, and F. W. Lichtenthaler, *Angew. Chem. Int. Ed. Engl.* **35** (1997).
- <sup>80</sup> A. Laio and M. Parrinello, *Proc. Natl. Acad. Sci. USA* **99**, 12562 (2002).
- <sup>81</sup> M. Iannuzzi, A. Laio, and M. Parrinello, *Phys. Rev. Lett.* **90**, 238302 (2003).
- <sup>82</sup> A. Laio, A. Rodriguez-Fortea, F. Gervasio, M. Ceccarelli, and M. Parrinello, *J. Phys. Chem. B* **109**, 6714 (2005).
- <sup>83</sup> G. Bussi, A. Laio, and M. Parrinello, *Phys. Rev. Lett.* **96**, 90601 (2006).
- <sup>84</sup> A. Laio and F. L. Gervasio, *Rep. Prog. Phys.* **71**, 126601 (2008).
- <sup>85</sup> T. Huber, A. Torda, and W. F. van Gunsteren, *J. Comput.-Aided Mol. Des.* **8**, 695 (1994).
- <sup>86</sup> M. Mezei, *J. Comput. Phys.* **68**, 237 (1987).
- <sup>87</sup> M. Bonomi, A. Barducci, and M. Parrinello, *J. Comput. Chem.* (2009).
- <sup>88</sup> H. L. Strauss and H. M. Pickett, *J. Am. Chem. Soc.* **92**, 7281 (1970).
- <sup>89</sup> N. Zefirov, V. Palyulin, and E. Dashevskaya, *J. Phys. Org. Chem.* **3**, 147 (1990).
- <sup>90</sup> C. Haasnoot, *J. Am. Chem. Soc.* **114**, 882 (1992).
- <sup>91</sup> A. Bérces, D. Whitfield, and T. Nukada, *Tetrahedron* **57**, 477 (2001).
- <sup>92</sup> C. Camilloni, D. Provasi, G. Tiana, and R. A. Broglia, *Proteins* **71**, 1647 (2008).
- <sup>93</sup> H. J. C. Berendsen, D. van der Spoel, and R. van Drunen, *Comput. Phys. Comm.* **91**, 43 (1995).
- <sup>94</sup> E. Lindahl, B. Hess, and D. van der Spoel, *J. Mol. Mod.* **7**, 306 (2001).
- <sup>95</sup> D. van der Spoel, E. Lindahl, B. Hess, G. Groenhof, A. E. Mark, and H. J. C. Berendsen, *J. Comput. Chem.* **26**, 1701 (2005).
- <sup>96</sup> H. J. C. Berendsen, J. P. M. Postma, A. DiNola, and J. R. Haak, *J. Chem. Phys.* **81**, 3684 (1984).
- <sup>97</sup> S. Miyamoto and P. A. Kollman, *J. Comput. Chem.* **13**, 952 (1992).
- <sup>98</sup> J. Ryckaert, G. Ciccotti, and H. Berendsen, *J. Comput. Phys.* **23**, 327 (1977).
- <sup>99</sup> S. Nosé, *Mol. Phys.* **52**, 255 (1984).
- <sup>100</sup> W. Hoover, *Phys. Rev. A* **31**, 1695 (1985).
- <sup>101</sup> M. Parrinello and A. Rahman, *J. Appl. Phys.* **52**, 7182 (1981).

<sup>102</sup> See Supplementary Material Document No. for the full gromacs topologies of all pyranoses using the new parameter set.

## List of Figures

- 1 Numbering scheme for aldopyranoses rings. . . . . 32
- 2 Schematic representation of stable ring conformers, located on the  $(\theta, \phi)$  plane of Cremer–Pople coordinates: chair (a) ; inverted chair (b) boats (c and e) ; skew boats (e and f). Exact chair conformers ( $\theta = 0$ ,  $\theta = \pi$ ) have been represented out of the plane, to underline that for them the  $\phi$  angle is not defined. . . . . 33
- 3 Puckering free energy landscape (already corrected with the results from the umbrella sampling phase) of  $\beta$ -D-Glc using the standard 45a4 parameter set. Upper panel: the  $(\theta, \phi)$  plane is shown, with isolines drawn every 10 kJ/mol starting from the absolute minimum. Lower panel: projection of the free energy profile onto the  $\phi = 0$  plane. Darker colors correspond to lower energies. . 34
- 4 Contribution to the total puckering free energy of  $\beta$ -D-Glc (45a4 parameters) from the equilibrium sampling,  $-k_B T \ln \rho_{\text{bias}}(\theta, \phi)$ . An immaterial constant has been added, so that the correction term is zero at the position of the free energy global minimum. Isolines are drawn every 2.5 kJ/mol (upper panel). The projection onto the  $\phi = 0$  plane of the correction term (lower panel). . . . . 35
- 5 Inverted chair free energy difference for the  $\beta$  (upper panel) and  $\alpha$  (lower panel) series of aldopyranoses. The three curves refer to the simulation results obtained using the 45a4 parameter set (squares) and the predictions of Ref. 61 (triangles) and Ref. 62 (circles). Diamonds corresponds to the estimates from NMR measurements (idose, Ref.50; altrose, this work). Lines are a guide to the eye, and error bars are always smaller than the symbols (0.5 kJ/mol). . . . 36
- 6 Results of the unbiased molecular dynamics simulation of  $\beta$ -D-Glc. Histogram of the population along the  $\theta$  puckering coordinate (upper panel) and time evolution of the number of inverted chairs (lower panel). . . . . 37

7	Inverted chair free energy difference for the $\beta$ (upper panel) and $\alpha$ (lower panel) series of aldopyranoses. The three curves refer to the simulation results using the new parameter set (squares) and the predictions of Ref. 61 (triangles) and Ref. 62 (circles). Diamonds corresponds to the estimates from NMR measurements (idose, Ref.50; altrose, this work). Lines are a guide to the eye, and error bars are always smaller than the symbols (0.5 kJ/mol). . . .	38
8	Puckering free energy landscapes (in kJ/mol) obtained by the combined metadynamics – umbrella sampling, for the series of $\beta$ -D-aldopyranoses simulated using the new force field parameters. Isolines are drawn every 10 kJ/mol, starting from the global minimum. . . . .	39
9	Puckering free energy landscapes (in kJ/mol) obtained by the combined metadynamics – umbrella sampling, for the series of $\alpha$ -D-aldopyranoses simulated using the new force field parameters. Isolines are drawn every 10 kJ/mol, starting from the global minimum. . . . .	40

**List of Tables**

I	Orientation of ring substituents (ax: axial; eq: equatorial) for different stereoisomers (referred to the ${}^4C_1$ conformer). . . . .	42
II	Assigned chemical shifts and coupling constants for the four main forms of altropyranose. . . . .	43
III	Free energy and population of different conformers using the 45a4 parameter set. . . . .	44
IV	New parameters for D-aldopyranoses torsional interactions. . . . .	45
V	Free energy and population of different conformers using the new parameter set. . . . .	46

## Figures

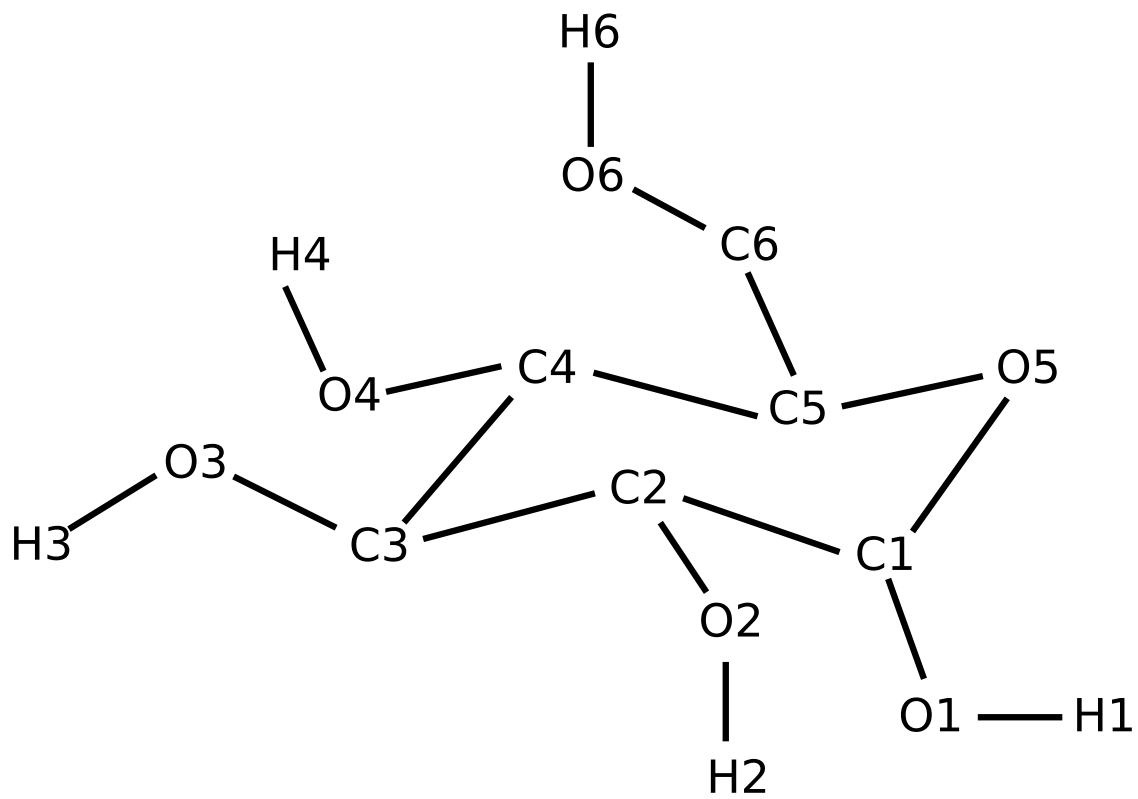


FIG. 1:

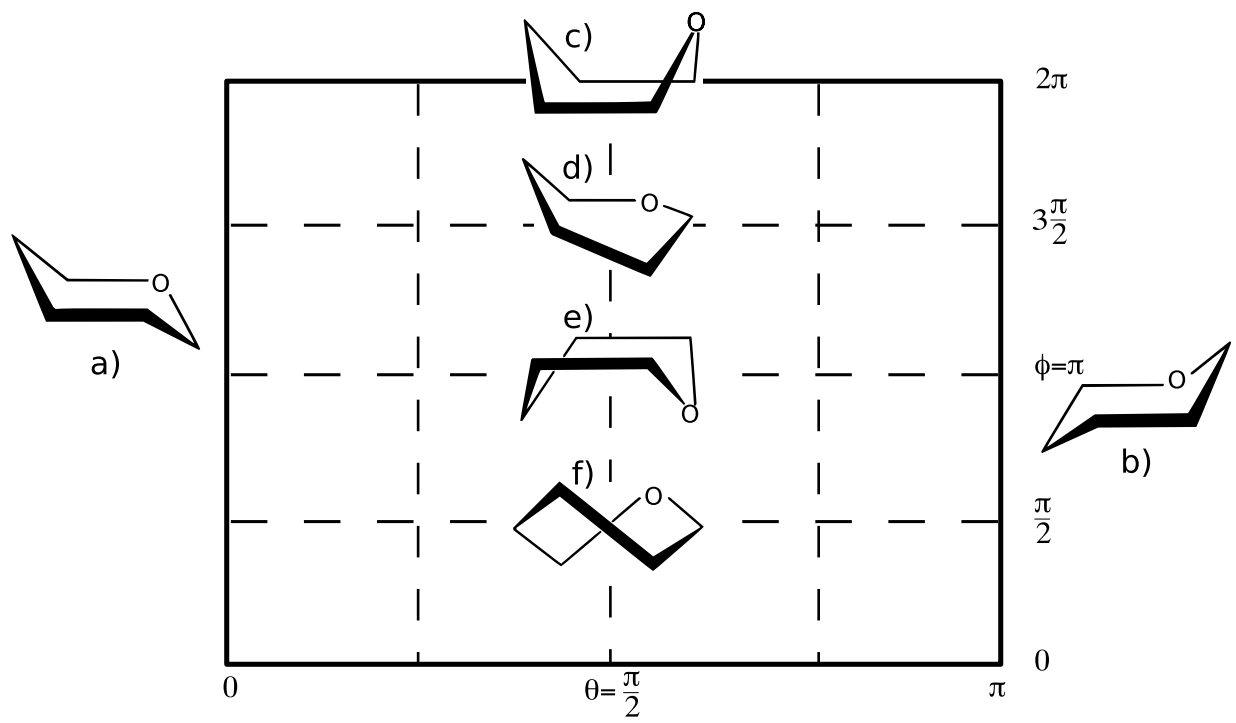


FIG. 2:

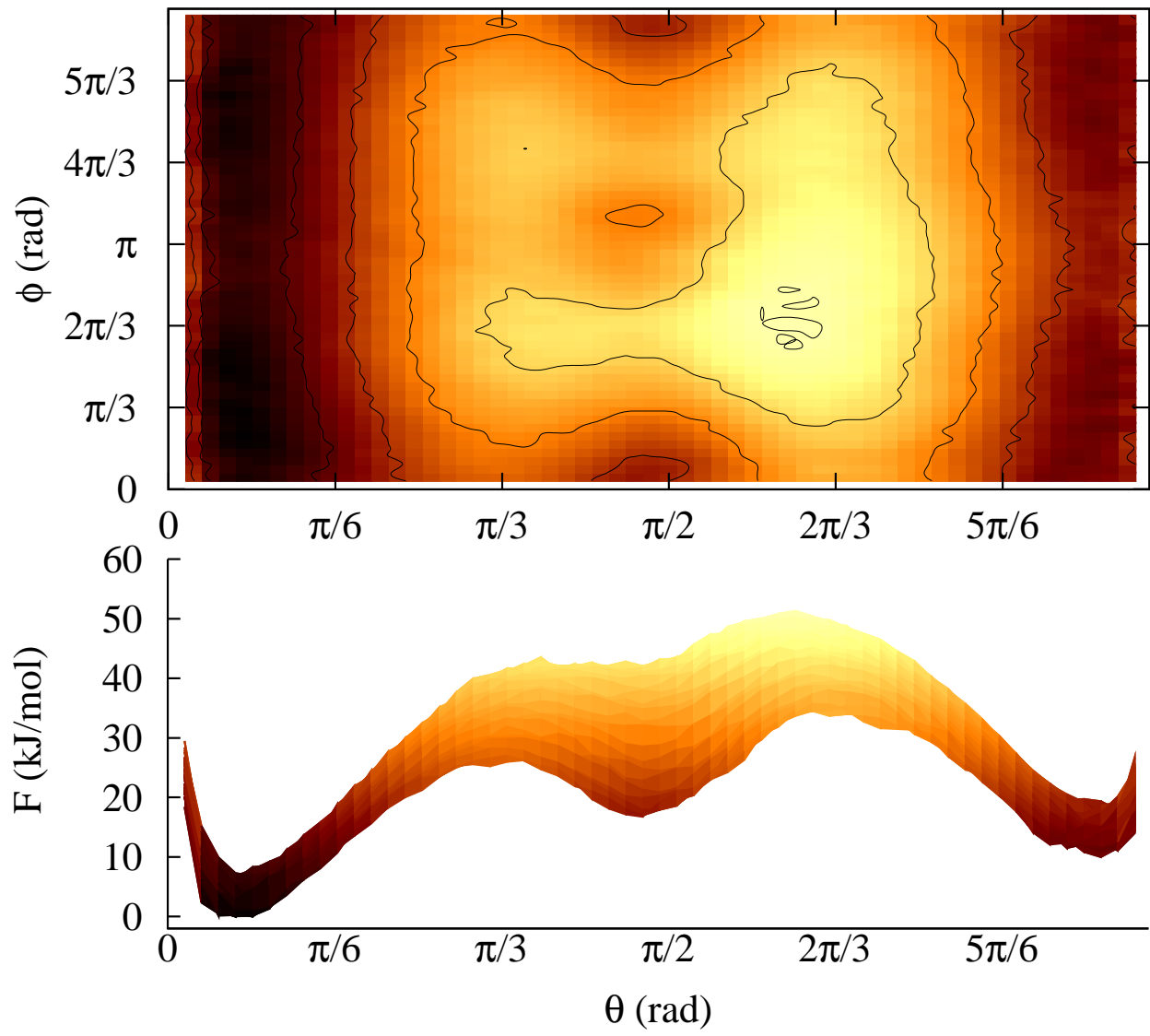


FIG. 3:

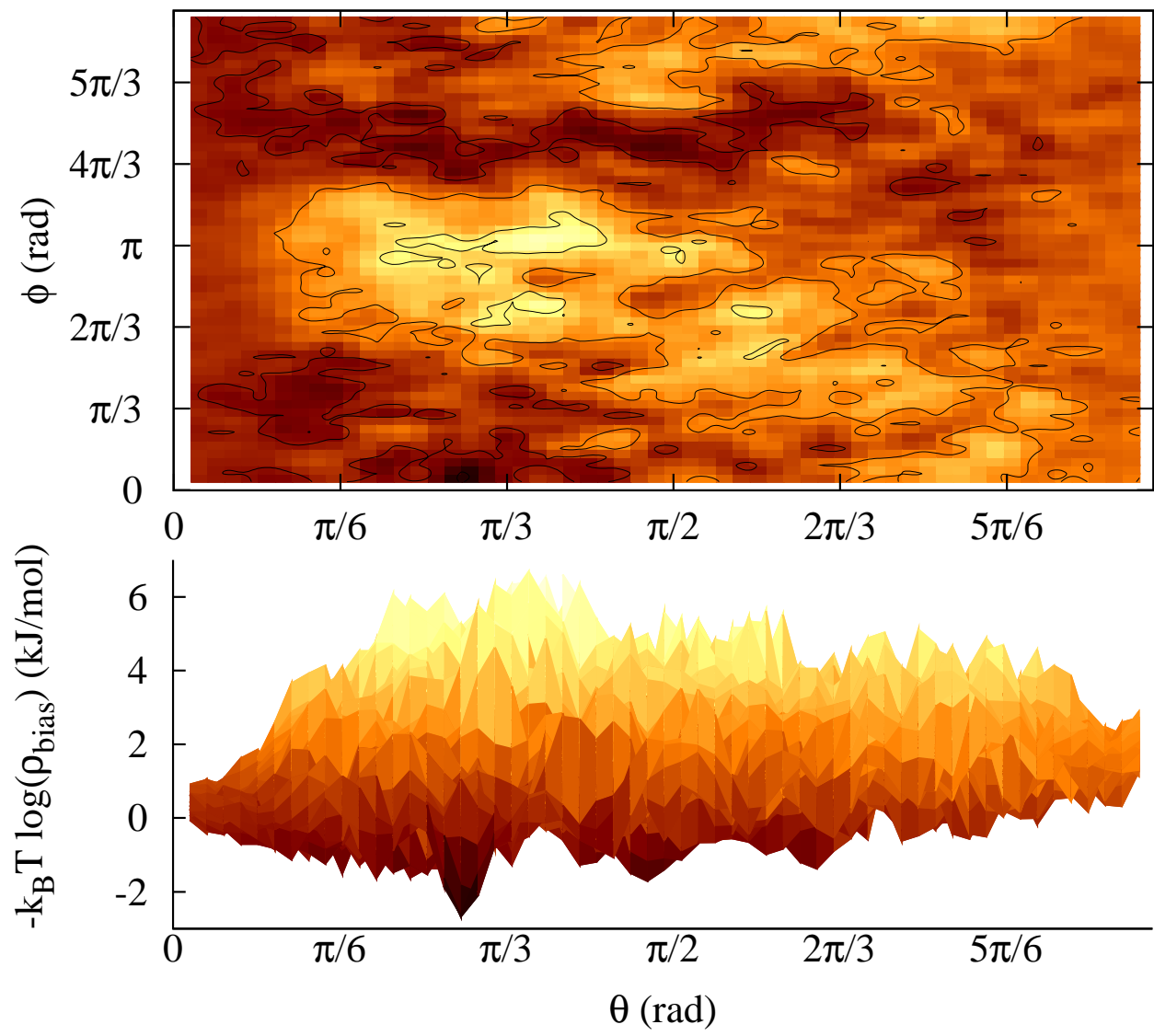


FIG. 4:

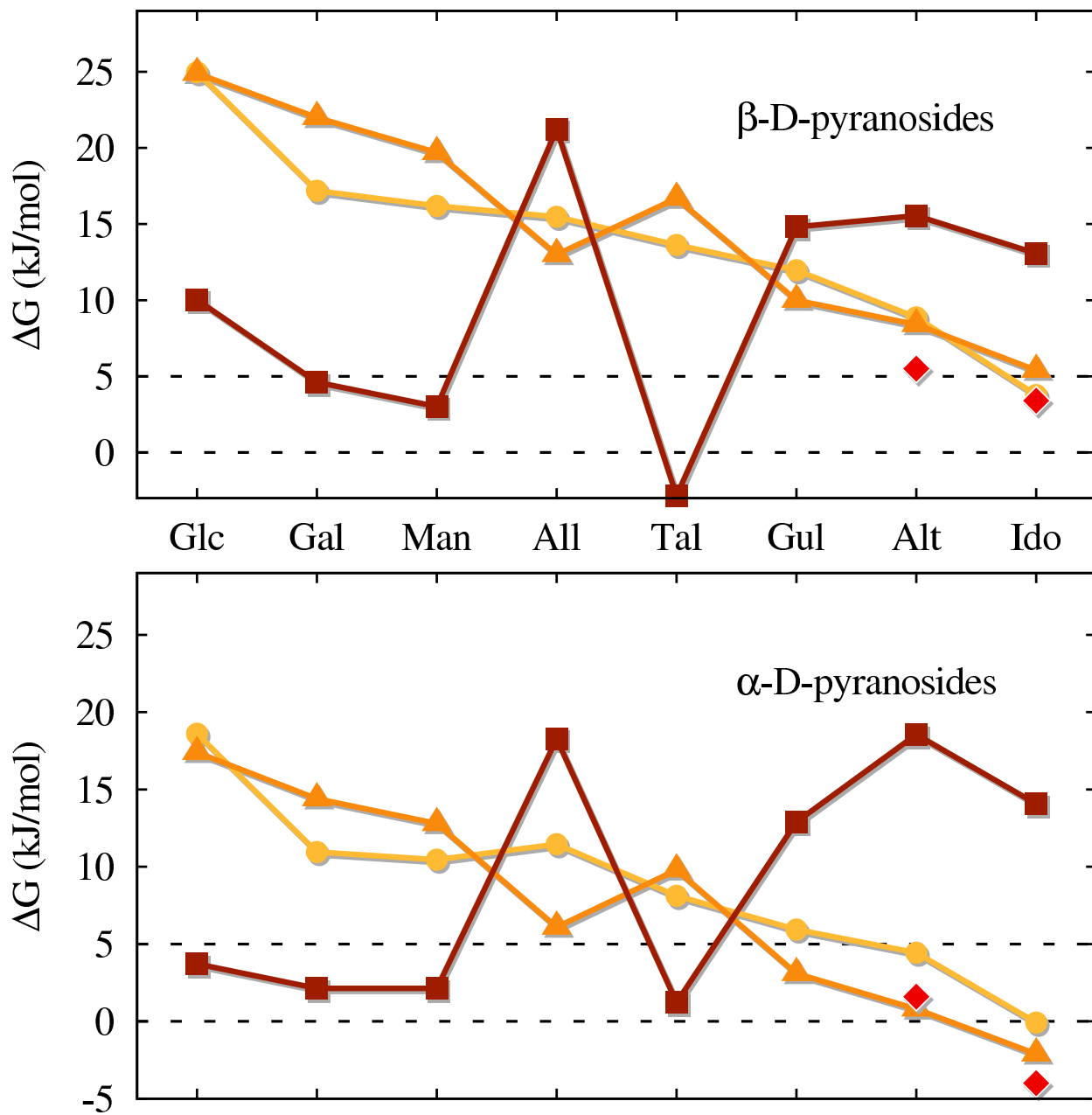


FIG. 5:

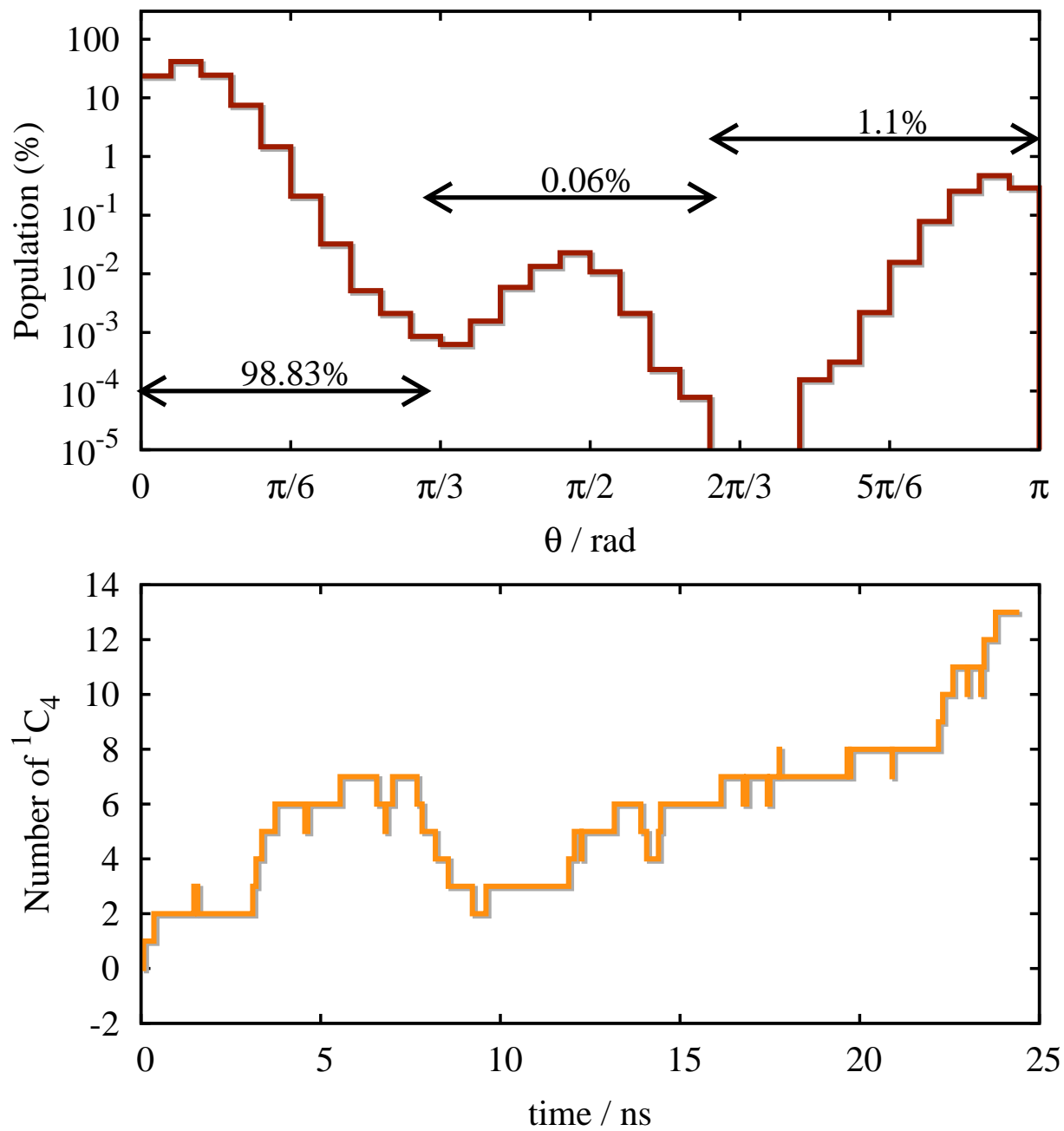


FIG. 6:

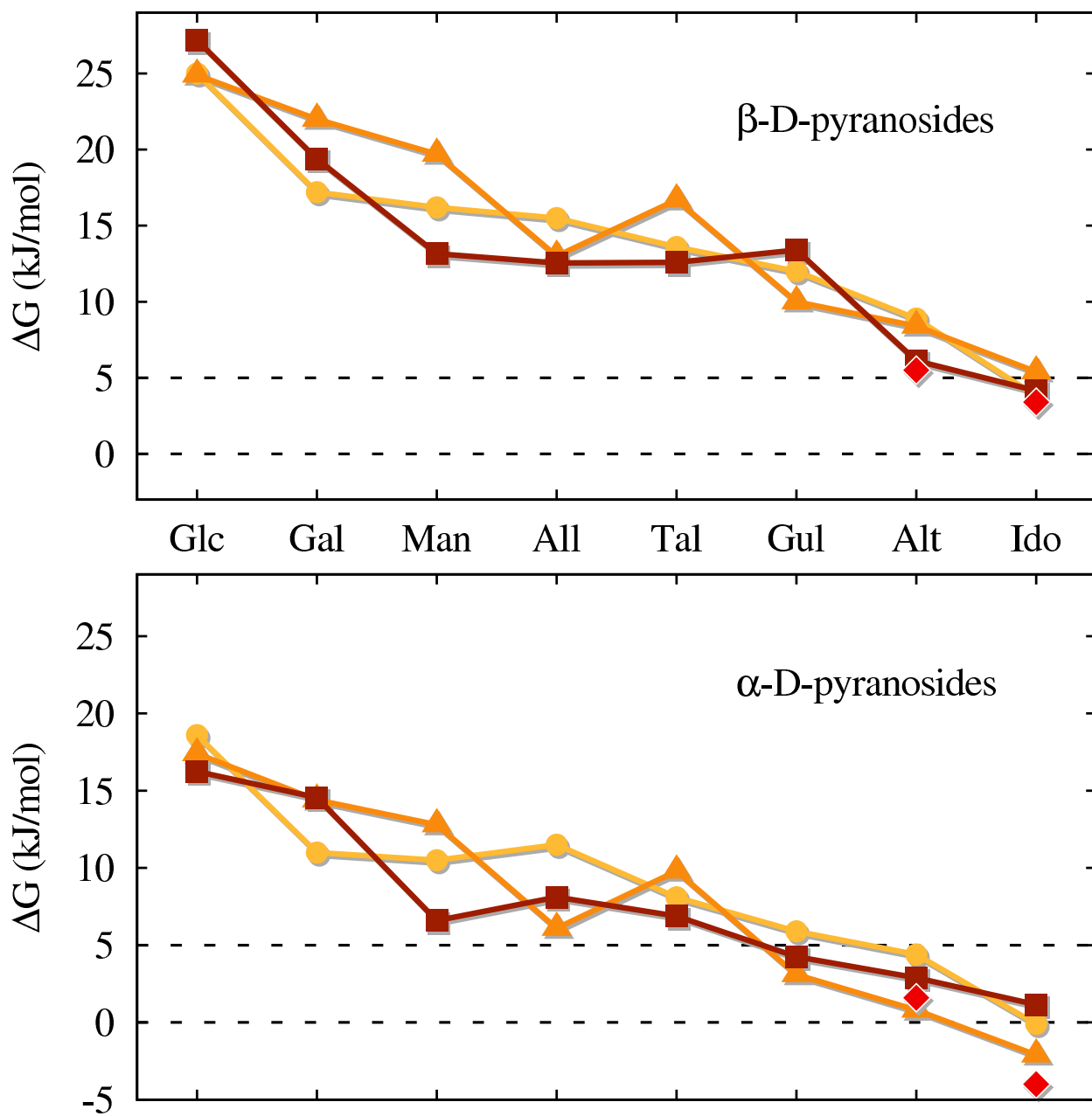


FIG. 7:

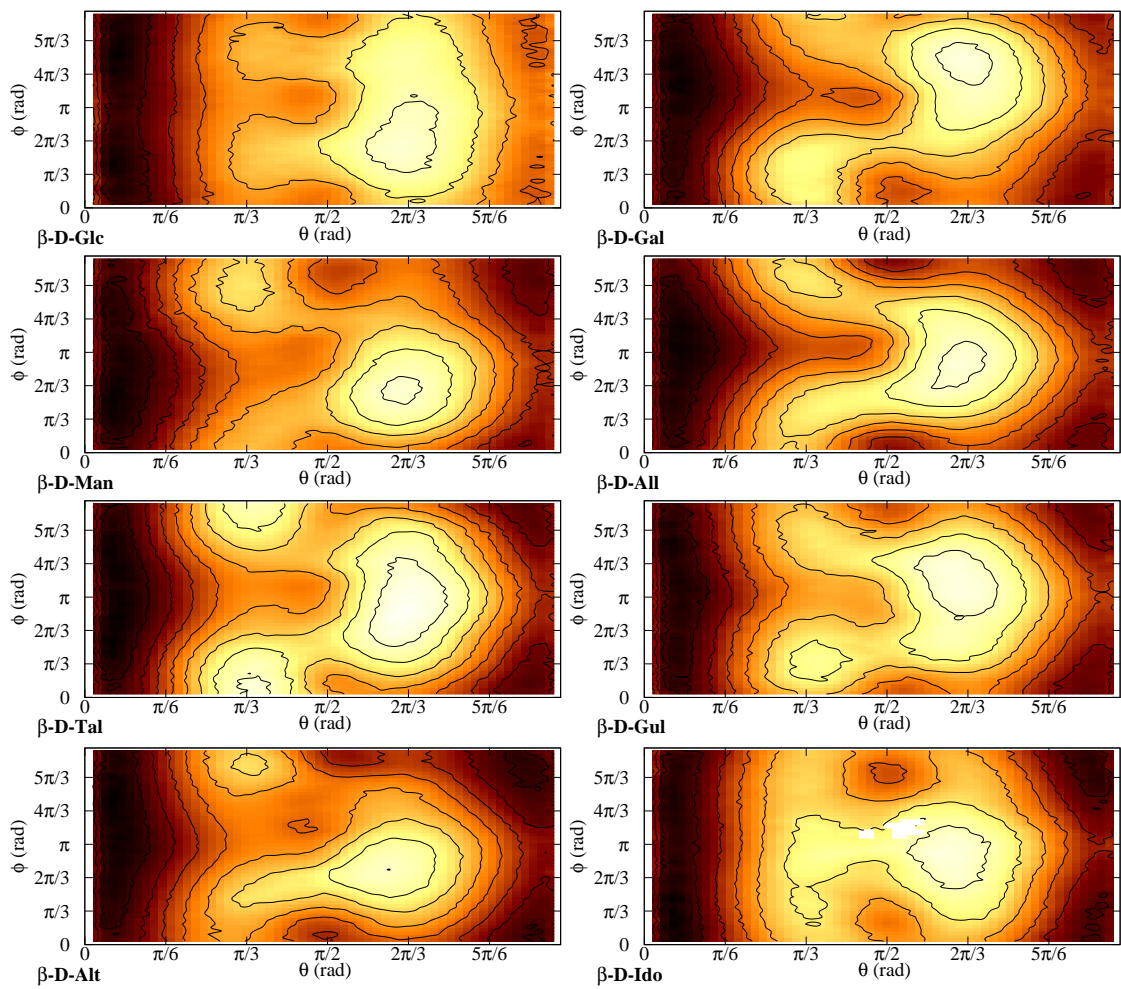


FIG. 8:

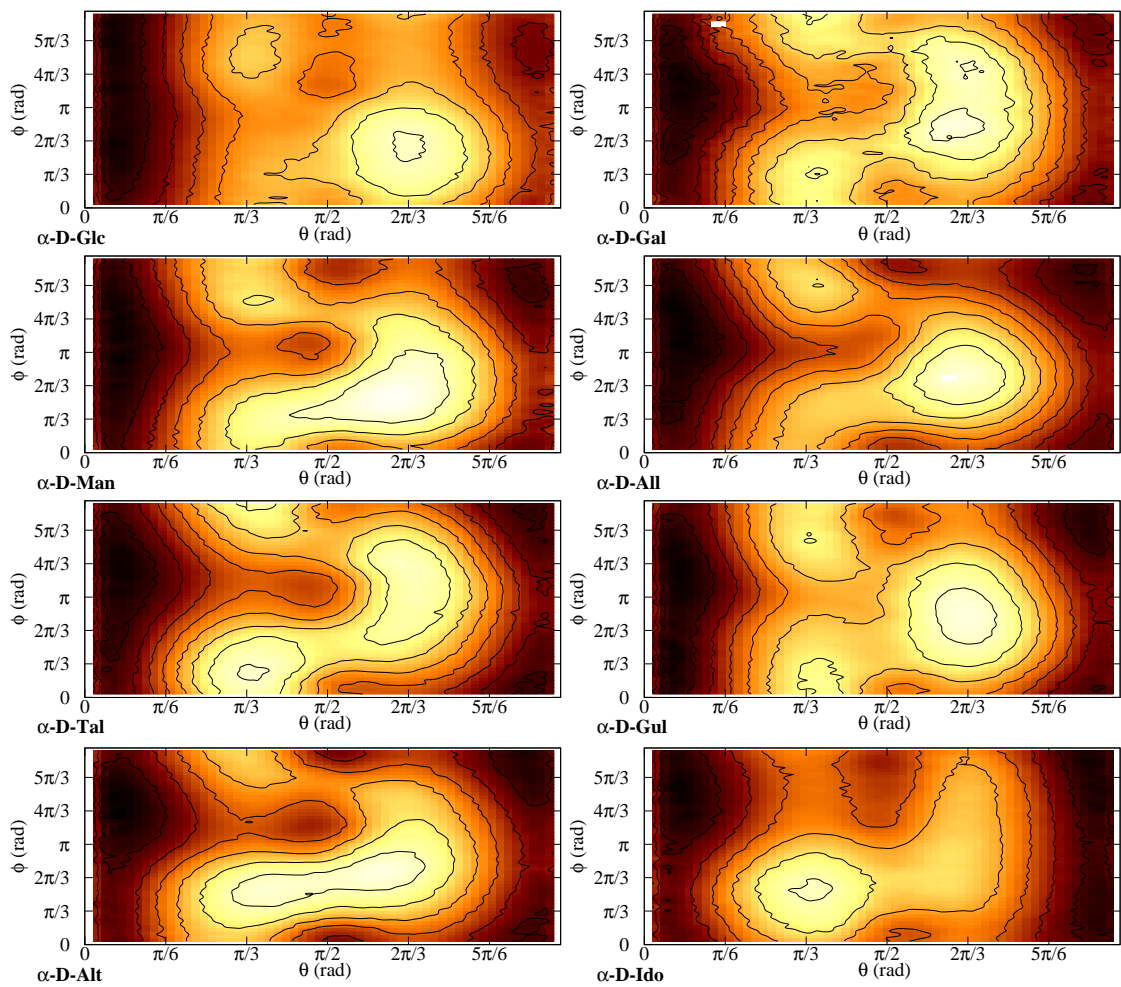


FIG. 9:

## Tables

Stereoisomer	C1	C2	C3	C4	C5
$\beta$ -D-Glc	eq	eq	eq	eq	eq
$\beta$ -D-Gal	eq	eq	eq	ax	eq
$\beta$ -D-Man	eq	ax	eq	eq	eq
$\beta$ -D-All	eq	eq	ax	eq	eq
$\beta$ -D-Tal	eq	ax	eq	ax	eq
$\beta$ -D-Gul	eq	eq	ax	ax	eq
$\beta$ -D-Alt	eq	ax	ax	eq	eq
$\beta$ -D-Ido	eq	ax	ax	ax	eq

TABLE I: Orientation of ring substituents (ax: axial; eq: equatorial) for different stereoisomers (referred to the  ${}^4C_1$  conformer).

H/C Type	$\alpha$ -D-altropyranose						$\beta$ -D-altropyranose					
	$\delta_H^a$	$\delta_C^a$	${}^3J_{HH}^a$	$\delta_H^b$	$\delta_C^b$	${}^3J_{HH}^b$	$\delta_H^a$	$\delta_C^a$	${}^3J_{HH}^a$	$\delta_H^b$	$\delta_C^b$	${}^3J_{HH}^b$
H <sub>1</sub> /C <sub>1</sub>	5.01	95.3	3.4+W <sub>1-3</sub>	4.93	96.3	1.5+W <sub>1-3</sub>	5.14	93.3	1.4+W <sub>1-5</sub>	5.04	93.5	1.3+W <sub>1-5</sub>
H <sub>2</sub> /C <sub>2</sub>	3.87	71.9	3.4, 5.6	3.81	71.4	1.5, 3.6	3.85	72.3	1.4, 4.1	3.69	73.1	1.3, 3.9
H <sub>3</sub> /C <sub>3</sub>	3.95	71.8	3.7, 5.6	3.88	72.9	3.0, 3.6	3.83	75.6	2.2, 4.1	3.95	72.7	3.0, 3.9
H <sub>4</sub> /C <sub>4</sub>	3.91	66.8	3.7, 7.6	3.80	65.6	3.0, 9.8	3.84	65.6	2.2, 9.1	3.74	66.0	3.0, 9.8
H <sub>5</sub> /C <sub>5</sub>	4.09	72.8	3.4, 6.3, 7.4	3.98	70.5	2.7, 5.5, 9.8	4.08	72.1	2.2, 4.9, 9.1	3.70	75.8	2.0, 5.5, 9.8
H <sub>6</sub> /C <sub>6</sub>	3.81	62.1	6.3, 12.0	3.75	63.2	5.5, 11.8	3.75	63.1	2.2, 11.7	3.67	63.6	5.5, 11.7
H <sub>6'</sub> /C <sub>6</sub>	3.83		3.4, 12.0	3.83		2.7, 11.8	3.90		4.9, 11.7	3.81		2.0, 11.7

Chemical shifts of  ${}^{13}\text{C}$  ( $\delta_C$ ) and  ${}^1\text{H}$  ( $\delta_H$ ) are reported in ppm; coupling constants are reported in Hz.

<sup>a</sup> in D<sub>2</sub>O; <sup>b</sup> in CD<sub>3</sub>OD.

TABLE II: Assigned chemical shifts and coupling constants for the four main forms of altropyranose.

Isomer	$\Delta G$ [ ${}^1C_4$ ] <sup>a</sup>	Next <sup>b</sup>	$\Delta G$ [Next] <sup>c</sup>	TS <sup>d</sup>	$\Delta G$ [TS] <sup>e</sup>	P[ ${}^4C_1$ ] <sup>f</sup>	P[ ${}^1C_4$ ] <sup>g</sup>	P[Next] <sup>h</sup>
$\beta$ -D-Glc	$10.0 \pm 0.2$	${}^3O_B$	$16.7 \pm 0.2$	(1.06,0.10)	$25.9 \pm 0.2$	98.42(1)	1.52(1)	$4.6(1) \times 10^{-2}$
$\beta$ -D-Gal	$4.6 \pm 0.2$	${}^3S_1$	$21.5 \pm 0.2$	(1.11,3.94)	$38.6 \pm 0.4$	91.2(1)	8.8(1)	$6.2(1) \times 10^{-3}$
$\beta$ -D-Man	$3.0 \pm 0.2$	${}^OS_2$	$23.2 \pm 0.2$	(1.11,2.44)	$41.2 \pm 0.2$	80.6(1)	19.4(1)	$4.3(1) \times 10^{-3}$
$\beta$ -D-All	$21.2 \pm 0.2$	${}^3O_B$	$27.9 \pm 0.2$	(1.17,3.40)	$36.9 \pm 0.3$	99.98(1)	0.0205(2)	$4.6(1) \times 10^{-4}$
$\beta$ -D-Tal	$-2.8 \pm 0.2$	${}^3O_B$	$36.8 \pm 0.2$	(1.11,3.62)	$47.6 \pm 0.2$	58.7(2)	41.3(1)	$3.8(1) \times 10^{-5}$
$\beta$ -D-Gul	$14.8 \pm 0.3$	${}^OS_2$	$33.9 \pm 0.1$	(1.22,3.30)	$43.2 \pm 0.2$	99.92(1)	0.08(1)	$5.7(1) \times 10^{-5}$
$\beta$ -D-Alt	$15.5 \pm 0.2$	${}^OS_2$	$33.7 \pm 0.1$	(1.11,3.94)	$42.4 \pm 0.2$	99.87(1)	0.129(2)	$9.4(1) \times 10^{-5}$
$\beta$ -D-Ido	$13.0 \pm 0.2$	$B_{25}$	$35.0 \pm 0.3$	(1.06,4.47)	$44.9 \pm 0.1$	99.59(1)	0.412(4)	$6.1(1) \times 10^{-5}$
$\alpha$ -D-Glc	$3.7 \pm 0.2$	${}^OS_2$	$25.7 \pm 0.2$	(1.11,0.21)	$35.2 \pm 0.2$	90.85(6)	9.15(7)	$1.7(1) \times 10^{-3}$
$\alpha$ -D-Gal	$2.1 \pm 0.2$	${}^3S_1$	$33.0 \pm 0.2$	(1.11,3.40)	$47.1 \pm 0.2$	74.9(2)	25.1(2)	$5.8(1) \times 10^{-5}$
$\alpha$ -D-Man	$2.3 \pm 0.3$	${}^OS_2$	$15.2 \pm 0.3$	(1.11,3.30)	$29.5 \pm 0.4$	71.9(3)	28.0(2)	$3.9(1) \times 10^{-2}$
$\alpha$ -D-All	$18.2 \pm 0.2$	${}^3O_B$	$35.6 \pm 0.2$	(1.65,4.79)	$56.6 \pm 0.3$	99.94(1)	0.060(1)	$3.4(1) \times 10^{-5}$
$\alpha$ -D-Tal	$1.2 \pm 0.3$	${}^1S_3$	$32.1 \pm 0.3$	(1.11,3.51)	$37.1 \pm 0.3$	63.7(4)	36.3(3)	$3.0(1) \times 10^{-4}$
$\alpha$ -D-Gul	$12.9 \pm 0.2$	${}^OS_2$	$42.7 \pm 0.2$	(1.06,3.72)	$30.5 \pm 0.2$	99.49(1)	0.51(1)	$7.0(1) \times 10^{-6}$
$\alpha$ -D-Alt	$18.5 \pm 0.4$	${}^OS_2$	$23.1 \pm 0.2$	(1.17,2.87)	$45.5 \pm 0.3$	99.93(1)	0.065(1)	$5.5(1) \times 10^{-3}$
$\alpha$ -D-Ido	$14.0 \pm 0.2$	${}^1S_3$	$27.9 \pm 0.2$	(1.11,4.36)	$33.6 \pm 0.2$	99.47(1)	0.524(3)	$1.4(1) \times 10^{-3}$

Energies are expressed in kJ/mol, angles are in rad, and probabilities in percent; <sup>a</sup> Free energy of  ${}^1C_4$ ; <sup>b</sup>

Next most populated conformer after  ${}^4C_1$  and  ${}^1C_4$ ; <sup>c</sup> Free energy of the next most populated conformer; <sup>d</sup>

Location of the transition state ( $\theta, \phi$ ); <sup>e</sup> Free energy of the transition state ; <sup>f</sup> Population of  ${}^4C_1$  (%); <sup>g</sup>

Population of  ${}^1C_4$  (%); <sup>h</sup> Population of the next most populated conformer. When a basin is present,

which encompasses many states, all conformers involved are listed.

TABLE III: Free energy and population of different conformers using the 45a4 parameter set.

dihedral angle	$k_\phi$ <sup>§</sup>	$\cos \delta$	$n$
C3–C2–C1–O1 <sup>†</sup>	0.5	–1	2
C4–C3–C2–O2 <sup>†</sup>	0.5	–1	2
C1–C2–C3–O3 <sup>†</sup>	2.4	–1	2
C5–C4–C3–O3 <sup>†</sup>	2.4	–1	2
C1–O5–C5–C6 <sup>‡</sup>	0.5	–1	2

<sup>§</sup> in kJ/mol; <sup>†</sup> interaction modified with respect to the correspondent 45a4 one; <sup>‡</sup> new interaction term (not present in 45a4); The functional form for the torsional interaction is that of Eq.10. All other interactions are the same as in the 45a4 set<sup>35</sup>.

TABLE IV: New parameters for D-aldopyranoses torsional interactions.

Isomer	$\Delta G$ [ ${}^1C_4$ ] <sup>a</sup>	Next <sup>b</sup>	$\Delta G$ [Next] <sup>c</sup>	TS <sup>d</sup>	$\Delta G$ [TS] <sup>e</sup>	P[ ${}^4C_1$ ] <sup>f</sup>	P[ ${}^1C_4$ ] <sup>g</sup>	P[Next] <sup>h</sup>
$\beta$ -D-Glc	$27.1 \pm 0.3$	${}^3O_B$	$30.9 \pm 0.2$	(1.17,3.19)	$45.9 \pm 0.5$	99.99(1)	0.002(1)	$4.17(4) \times 10^{-4}$
$\beta$ -D-Gal	$19.3 \pm 0.2$	${}^3S_1$	$35.6 \pm 0.2$	(1.17,3.51)	$39.7 \pm 0.2$	99.95(1)	0.051(1)	$8.8(1) \times 10^{-5}$
$\beta$ -D-Man	$13.1 \pm 0.4$	${}^O S_2$	$32.9 \pm 0.4$	(1.17,2.66)	$42.7 \pm 0.5$	99.58(1)	0.42(1)	$1.41(3) \times 10^{-4}$
$\beta$ -D-All	$12.5 \pm 0.2$	${}^3O_B$	$21.8 \pm 0.2$	(1.22,3.19)	$36.8 \pm 0.3$	99.31(1)	0.68(1)	$9.23(1) \times 10^{-3}$
$\beta$ -D-Tal	$11.9 \pm 0.3$	$B_{30}$	$43.2 \pm 0.1$	(1.11,3.40)	$46.8 \pm 0.2$	99.53(1)	0.47(1)	$3.0(1) \times 10^{-6}$
$\beta$ -D-Gul	$13.3 \pm 0.3$	${}^O S_2$	$31.5 \pm 0.4$	(1.17,3.19)	$45.9 \pm 0.5$	99.00(2)	0.99(1)	$3.4(1) \times 10^{-4}$
$\beta$ -D-Alt	$6.1 \pm 0.1$	${}^O S_2$	$24.7 \pm 0.1$	(1.17,3.72)	$43.8 \pm 0.2$	93.88(4)	6.12(4)	$2.4(1) \times 10^{-3}$
$\beta$ -D-Ido	$4.1 \pm 0.3$	$B_{25}$	$27.4 \pm 0.2$	(1.06,5.85)	$44.9 \pm 0.2$	88.51(9)	11.5(2)	$8.6(1) \times 10^{-4}$
$\alpha$ -D-Glc	$16.2 \pm 0.2$	${}^1S_3-{}^{14}B$	$35.1 \pm 0.2$	(1.22,2.66)	$42.5 \pm 0.2$	99.88(1)	0.124(1)	$8.6(1) \times 10^{-5}$
$\alpha$ -D-Gal	$14.5 \pm 0.2$	${}^1S_3$	$44.7 \pm 0.2$	(1.22,3.19)	$48.5 \pm 0.4$	99.58(1)	0.416(5)	$4.0(1) \times 10^{-6}$
$\alpha$ -D-Man	$6.5 \pm 0.2$	${}^O S_2$	$22.8 \pm 0.1$	(1.11,3.19)	$32.3 \pm 0.3$	95.72(3)	4.27(5)	$6.0(1) \times 10^{-3}$
$\alpha$ -D-All	$8.1 \pm 0.2$	$B_{30}-{}^1S_3$	$27.1 \pm 0.2$	(1.17,3.40)	$38.9 \pm 0.2$	97.92(2)	2.08(3)	$8.7(1) \times 10^{-4}$
$\alpha$ -D-Tal	$6.8 \pm 0.1$	${}^O S_2$	$33.7 \pm 0.2$	(1.65,4.47)	$52.5 \pm 0.2$	91.60(6)	8.40(6)	$1.7(1) \times 10^{-4}$
$\alpha$ -D-Gul	$4.2 \pm 0.2$	${}^O S_2$	$30.3 \pm 0.2$	(1.49,3.94)	$49.2 \pm 0.3$	90.44(7)	9.6(1)	$1.2(1) \times 10^{-4}$
$\alpha$ -D-Alt	$2.8 \pm 0.3$	$B_{30}$	$15.0 \pm 0.2$	(1.06,3.72)	$28.9 \pm 0.2$	79.2(1)	20.7(2)	$8.74(1) \times 10^{-2}$
$\alpha$ -D-Ido	$1.1 \pm 0.2$	${}^O S_2-{}^{14}B$	$20.6 \pm 0.2$	(1.11,5.53)	$31.6 \pm 0.2$	51.8(3)	48.2(2)	$1.38(1) \times 10^{-2}$

Energies are expressed in kJ/mol, angles are in rad, and probabilities in percent; <sup>a</sup> Free energy of  ${}^1C_4$ ; <sup>b</sup>

Next most populated conformer after  ${}^4C_1$  and  ${}^1C_4$ ; <sup>c</sup> Free energy of the next most populated conformer; <sup>d</sup>

Location of the transition state ( $\theta, \phi$ ); <sup>e</sup> Free energy of the transition state ; <sup>f</sup> Population of  ${}^4C_1$  (%); <sup>g</sup>

Population of  ${}^1C_4$  (%); <sup>h</sup> Population of the next most populated conformer. When a basin is present,

which encompasses many states, all conformers involved are listed.

TABLE V: Free energy and population of different conformers using the new parameter set.